Published in final edited form as:
Dev Biol. 2011 December 1; 360(1): 30–43. doi:10.1016/j.ydbio.2011.09.004.

Rac1 GTPase -deficient mouse lens exhibits defects in shape, suture formation, fiber cell migration and survival

Rupalatha Maddala[a], **Bharesh K. Chauhan**[b], **Christopher Walker**[a], **Yi Zheng**[c], **Michael L. Robinson**[d], **Richard A. Lang**[b,*], and **Ponugoti V. Rao**[a,e,*]

[a]Department of Ophthalmology, Duke University School of Medicine, Durham, NC. USA

[b]The Visual System Group, Division of Pediatric Ophthalmology and Developmental Biology, Children's Hospital Research Foundation, University of Cincinnati, Cincinnati, OH. USA

[c]Division of Experimental Hematology, Children's Hospital Research Foundation, University of Cincinnati, Cincinnati, OH. USA

[d]Department of Zoology, Miami University, Oxford, OH. USA

[e]Department of Pharmacology and Cancer Biology, Duke University School of Medicine, Durham, NC. USA

Abstract

Morphogenesis and shape of the ocular lens depend on epithelial cell elongation and differentiation into fiber cells, followed by the symmetric and compact organization of fiber cells within an enclosed extracellular matrix-enriched elastic capsule. The cellular mechanisms orchestrating these different events however, remain obscure. We investigated the role of the Rac1 GTPase in these processes by targeted deletion of expression using the conditional gene knockout (cKO) approach. Rac1 cKO mice were derived from two different Cre (Le-Cre and MLR-10) transgenic mice in which lens-specific Cre expression starts at embryonic day 8.75 and 10.5, respectively, in both the lens epithelium and fiber cells. The Le-Cre/Rac1 cKO mice exhibited an early-onset (E12.5) and severe lens phenotype compared to the MLR-10/Rac1 cKO (E15.5) mice. While the Le-Cre/Rac1 cKO lenses displayed delayed primary fiber cell elongation, lenses from both Rac1 cKO strains were characterized by abnormal shape, impaired secondary fiber cell migration, sutural defects and thinning of the posterior capsule which often led to rupture. Lens fiber cell N-cadherin/β-catenin/Rap1/Nectin-based cell-cell junction formation and WAVE-2/Abi-2/Nap1-regulated actin polymerization were impaired in the Rac1 deficient mice. Additionally, the Rac1 cKO lenses were characterized by a shortened epithelial sheet, reduced levels of extracellular matrix (ECM) proteins and increased apoptosis. Taken together, these data uncover the essential role of Rac1 GTPase activity in establishment and maintenance of lens shape, suture formation and capsule integrity, and in fiber cell migration, adhesion and survival, via regulation of actin cytoskeletal dynamics, cell adhesive interactions and ECM turnover.

[*]***Correspondence*** P. Vasantha Rao, Ph.D, Department of Ophthalmology, AERI Building, Room 4010, Duke University School of Medicine, Durham, NC 27710, Phone: 919-681-5883, Fax: 919-684-8983, rao00011@mc.duke.edu, ***Co-correspondence*** Richard A. Lang, Ph.D, Department of Pediatric Ophthalmology, Children's Hospital Research Foundation, 3333 Burnet Avenue, Cincinnati, OH 45229, Phone: 513-636-2700, Fax: 513-803-0740, Richard.Lang@cchmc.org.

Keywords

Rac1 GTPase; lens fibers; conditional knockout; migration; cell adhesion

Introduction

Vertebrate lens morphogenesis, which is initiated from a single cell type, provides a unique model system to explore the interrelationship between epithelial cell elongation and differentiation into fiber cells, and the intercellular and cell: extracellular matrix adhesive interactions which drive the migration and symmetric packing arrangement of fiber cells (Chow and Lang, 2001; McAvoy, 1980). These key determinants of lens morphogenesis, architecture and ultimately its optical properties are thought to be regulated in part, by various intrinsic and extrinsic factors that control dynamic reorganization of the actin cytoskeleton and cell adhesive interactions (Bassnett et al., 1999; Beebe et al., 2001; Danysh and Duncan, 2009; Menko S., 2004; Quinlan, 2004; Rafferty and Scholz, 1991; Ramaekers et al., 1981; Rao and Maddala, 2006; Straub et al., 2003). Importantly, disruption of actin cytoskeletal organization and cell adhesive interactions have been shown to impair lens epithelial cell elongation and differentiation, underlining the importance of actin cytoskeletal organization and cell-cell interactions in these cellular processes (Beebe and Cerrelli, 1989; Cain et al., 2008; Maddala et al., 2004; Menko S., 2004; Mousa and Trevithick, 1977; Pontoriero et al., 2009; Weber and Menko, 2006a). Although important insights have emerged regarding the external cues which control lens epithelial cell proliferation and differentiation (Chow and Lang, 2001; Lovicu and McAvoy, 2005), little is known about the cellular signaling pathways regulating lens fiber cell actin cytoskeletal dynamics, migration, adhesion and shape (Chen et al., 2008; Cooper et al., 2008; Grove et al., 2004; Maddala et al., 2004; Maddala et al., 2008; Rivera et al., 2009; Weber and Menko, 2006a; Weber and Menko, 2006b; Zelenka, 2004). Therefore, to understand how a functional lens is formed from a single cell type and how this organ attains its distinct architecture, it is important to identify the molecular mechanisms that regulate the cytoarchitecture and adhesive interactions of lens epithelial and fiber cells.

Rho GTPases are GTP-binding proteins that play a pivotal role in regulating actin cytoskeletal organization, cell adhesive interactions, and influence cell polarity, morphogenesis, migration, vesicle trafficking, cell cycle progression and transcriptional activity (Burridge and Wennerberg, 2004; Etienne-Manneville and Hall, 2002; Ridley, 2001a; Ridley, 2011). Specific functions are attributed to the Rho, Rac and Cdc42 GTPases, with Rac GTPase regulating membrane ruffling, protrusive activity and lamellipodial formation via its effects on actin polymerization and cadherin-mediated cell–cell adhesion in various cell types (Burridge and Wennerberg, 2004; Etienne-Manneville and Hall, 2002; Fukata and Kaibuchi, 2001; Ridley, 2001a; Ridley, 2011). Mammals express three highly homologous Rac isoforms, Rac1, Rac2 and Rac3, with the ubiquitously expressed Rac1 being the best studied member of this family (Heasman and Ridley, 2008). Rac1 regulates actin dynamics through two main downstream effector pathways, one of which is comprised of the p21-activated kinase (PAK) which signals to the actin cytoskeleton via LIM kinase and cofilin (Bokoch, 2003; Yang et al., 1998). The second effector pathway involves the verprolin-homologous protein (WAVE), which is a member of the Wiskott-Aldrich syndrome protein (WASP) family (Eden et al., 2002; Ridley, 2011; Stradal et al., 2004; Takenawa and Suetsugu, 2007). Additionally, Rac and its exchange factor Tiam1 regulate cadherin/catenin-based cell-cell adhesion by facilitating translocation of cadherins to the adhesion site and stabilizing the adherens junctions (Fukata and Kaibuchi, 2001; Hordijk et al., 1997; Malliri and Collard, 2003; Takai et al., 2008).

Lens epithelial and fiber cells express Rac1 and Rac 2 GTPases (Maddala et al., 2001; Rao et al., 2004), and Rac GTPase activity is known to be stimulated by various growth factors, PI3 kinase and lipid oxides in lens epithelial cells (Girao et al., 2003; Maddala et al., 2003; Weber and Menko, 2006b). Further, the lens fiber cell plasma membrane has been shown to contain abundant levels of Rac GTPase relative to all other Rho family GTPases (Bassnett et al., 2009). Importantly, transgenic mouse lenses overexpressing Rho GDIα, a negative regulator of Rho GTPases, exhibit defects in development and tissue architecture (Maddala et al., 2008). Additional indirect evidence for the participation of Rac GTPase in lens fiber cell migration, adhesion and differentiation has also been documented in WNT/PCP (Chen et al., 2008) and Abi-2 (Grove et al., 2004) targeted and PI3-kinase (Weber and Menko, 2006b) inhibitor treated lenses.

While there is circumstantial evidence for the participation of Rac GTPase in lens fiber cell differentiation, migration and adhesion, its direct role in these events and lens morphogenesis remains to be defined. To explore this objective, we generated lens specific Rac1 cKO mouse models by suppressing Rac1 expression in distinct regions and at different stages of the developing lens. Collectively, these Rac1 cKO mouse models reveal that Rac1 plays a crucial role in establishment of lens shape, suture formation, fiber cell migration and survival via its effects on actin cytoskeletal dynamics, cell adhesive interactions and ECM turnover.

Materials and methods

Generation of lens conditional Rac1 GTPase null mice

The $Rac1^{flox}$, Le-Cre, MLR10-Cre and MLR39-Cre transgenic mice used in this study have been described previously (Ashery-Padan et al., 2000; Chen et al., 2009; Glogauer et al., 2003; Zhao et al., 2004). Briefly, the conditional $Rac1^{flox/flox}$ mice obtained from the Jackson Laboratory contain loxP sites flanking (floxed) exon 1 on a C57BL/6J background. Mice homozygous for this allele are viable, fertile, normal in size and do not display any physical or behavioral abnormalities. The Le-Cre transgenic mice used in this study express Cre recombinase at embryonic day 8.75 under the control of a Pax6 P0 enhancer/promoter, with Cre being expressed in both lens epithelium and fiber cells as well as other surface ectoderm-derived eye structures (Ashery-Padan et al., 2000). The MLR10-Cre mice used in this study express Cre at embryonic day10.5 in both the lens epithelium and fibers under the transcriptional control of the minimal αA-crystallin promoter, which has been modified by the insertion of a Pax6 consensus binding element (Zhao et al., 2004). MLR39-Cre mice start expressing Cre at embryonic day 12.5 mainly in the lens fibers via the minimal αA-crystallin promoter, with little to no activity being present in the lens epithelium (Zhao et al., 2004). MLR10-Cre and MLR39-Cre mice, which were on FVB background, were backcrossed to wild type C57BL/6J mice to generate Cre transgenic mice on the C57BL/6J background. Obtained Le-Cre mice were in the C57BL/6J background. Mice that were homozygous for a Rac1 allele ($Rac1^{flox/flox}$) were crossed with mice heterozygous for a floxed Rac1 allele ($Rac1^{flox/wild\ type}$) and expressing Cre recombinase in the lens to generate Rac1 GTPase conditional knockout (cKO) offspring. Mice carrying the Le-Cre transgene (Fig. 1A), MLR10-Cre transgene (Fig.1B) and the Rac1 floxed alleles were genotyped by PCR using tail DNA. Animals were housed in a pathogen-free vivarium and used in accordance with institutional policies approved by the Duke University Institutional Animal Care & Use Committee (IACUC).

Histological analysis

Embryonic heads (E12.5, 14.5, 15.5 and 17.5) and whole eyes (day1) of Rac1 cKO and wild type (WT) littermate mice were fixed in 50 mM cacodylate buffer (pH 7.2) containing 2.5%

glutaraldehyde, 4% sucrose and 2 mM $CaCl_2$ for 2 h, and transferred to 10% buffered formalin as described earlier by us (Maddala et al., 2004). The specimens were subsequently embedded in glycol methacrylate, sectioned (2-μm sections) using a JB-4 microtome and stained with hematoxylin and eosin (H&E). Micrographs were captured using a Zeiss Axio Imager equipped with Hamamatsu Orca ER monochrome CCD camera.

Immunofluorescence analyses

Tissue sections derived from both cryosectioning and paraffin embedding were used in immunofluorescence analyses as we described earlier (Maddala, 2011). The following primary antibodies were used with paraffin sections at a 1:200 dilution for 24 h at 4°C: Rac1 (monoclonal, 610651, BD Transduction Laboratories, San Jose, CA), N-cadherin (monoclonal, clone: 3b9, Invitrogen, Camarillo CA), β-catenin (monoclonal, c7082, Sigma-Aldrich, St Louis, MO), Rap1A/Rap1B (polyclonal, 2399, Cell Signaling Technologies, Danvers, MA) and Nectin-1 (polyclonal, SC-28639, Santa Cruz Biotechnology, CA). Air dried tissue cryosections were immunostained with the respective polyclonal antibodies to fibronectin, laminin, collagen IV (gift from Harold Erickson, Duke University), Abi-2 (gift from Ann Marie Pendergast, Duke University), WAVE2 (Millipore, AB4226, Temecula CA) and E-cadherin (Cell Signaling Technologies, 4065, Danvers, MA), all used at a dilution of 1:1000. After incubation with primary antibodies (both paraffin-embedded and cryo-preserved tissue sections), the slides were washed and incubated in the dark for 2 h at room temperature (RT), with either Alexa fluor 488 or 594 conjugated secondary antibodies (Invitrogen). Slides were mounted using Vector mount and nail polish and photographed using a Nikon Eclipse 90i confocal laser scanning microscope. For F-actin staining, the pre-blocked sections were labeled with phalloidin conjugated with tetra rhodamine isothiocyanate (TRITC) (500 ng/ml; Sigma-Aldrich) as described above. All representative immunofluorescence data reported in this study were based on a minimum of 3 to 6 tissue sections derived from three independent specimens per group.

Immunoblotting

To evaluate changes in levels of Rac1, WAVE-2, integrins (αvβ1 (ABCAM ab75472), αvβ3 (Santa Cruz Biotec, SC-7312), αvβ5 (Santa Cruz Biotec, SC-13588) and β1 (Millipore, 04-1109), phospho-cofilin (C8992 Sigma-Adrich), Abi-2 (ABCAM ab70144), Nap1 (Sigma-Aldrich, N3788), fibronectin, laminin, collagen IV, β-catenin, N-cadherin, Rap1A/Rap1B, Nectin-1, and β and γ crystallins (gifts from Sam Zigler, Johns Hopkins University) and β-tubulin (Sigma-Aldrich T5293) in Rac1 cKO lenses, 6–8 intact postnatal day 1 (P1) lenses were pooled from both the WT and MLR-10/Rac1cKO mice. Pooled lens samples were homogenized in 10 mM Tris buffer pH 7.4 containing 0.2 mM MgCl2, 5 mM N-ethylmaleimide, 2.0 mM Na3 Vo4, 10 mM NaF, 60 μM phenyl methyl sulfonyl fluoride (PMSF), 0.4 mM iodoacetamide, Protease inhibitor cocktail tablets (complete, Mini, EDTA-free REF 11836170001) and PhosSTOP Phosphatase Inhibitor Cocktail Tablets (REF 04906837001) (1each/10ml buffer, Roche (Basel, Switzerland)). Homogenates were centrifuged at 800×*g* for 10 min at 4 °C. Protein concentration was estimated in supernatants using the Bio-Rad reagent (Cat. 500-0006). This fraction was centrifuged further at 100,000xg for 1 h at 4 °C and the insoluble pellet derived was resuspended in the tissue homogenization buffer. This centrifugation step was repeated twice and the resultant pellets were pooled and suspended in homogenization buffer containing 5 M urea, 2 M thiourea and 2% CHAPs and used as the membrane enriched fraction. Equal amounts of protein derived from the lens homogenate (800×g supernatant) or membrane enriched insoluble fraction were resolved on SDS-PAGE gels, followed by electrophoretic transfer to nitrocellulose membrane as described earlier (Maddala, 2011). Immunoblots were developed by enhanced chemiluminescence (ECL), and scanned densitometrically using a FOTO DYNE Gel Doc

scanner equipped with TL100 software, Densitometry analyses were carried out using ImageJ software (Maddala, 2011).

TUNEL assay

In situ terminal transferase dUTP nick end labeling (TUNEL) staining was performed using an ApopTag Plus Fluorescein kit (Chemicon, S7111, Temecula, CA) to evaluate and compare apoptotic cell death in lens sections from Rac1 cKO and WT littermate mice as we described earlier (Maddala et al., 2008). Apoptotic cells were scored using a fluorescence microscope (Zeiss Axioplan-II).

Electron microscopy

For transmission electron microscope-based histological analysis, freshly enucleated eyes from the Le-Cre/Rac1 cKO (E15.5), MLR-10/Rac1 cKO (E17.5), and WT mice were fixed in 10% buffered formalin and processed as we described earlier (Maddala, 2011). Electron microscopic images were captured with a Jeol JEM-1400 transmission electron microscope equipped with an Orius CCD digital camera (JEOL, Tokyo, Japan).

Actin filament fluorescence quantification

Actin filament fluorescence was quantified using either ImageJ or Metamorph. Signal intensity profiles from phalloidin-labelled lens pit cryosections (one central cryosection for n=3 eyes) were generated using ImageJ. A line was drawn around the lens pit for each example, the signal intensity was then tabulated. The intensity profile data was normalized to the average Hoechst 33258 signal for each lens pit, and then normalized for lens pit size. An average intensity profile was then generated. Similar measurements were done for each of the developmental stages studied. In the case of Metamorph-based measurements, the average fluorescence was quantified as the mean pixel intensity per unit area within each region. The camera measures the intensity of each pixel and gives a grey-scale value between 0 and 4096. Each measurement was corrected for the background fluorescence. Imaging conditions were set constant for both WT and Rac1 mutant sections, and 12-bit images were captured with an image exposure time of 100 milliseconds. The background corrected pixel intensity values were exported into excel sheet and saved for further analysis. A minimum of four measurements from each of six sections derived from three independent specimens were used to calculate average pixel intensities for each developmental stages tested.

Capsule width and epithelial sheet length measurements

Capsule width was measured using the measurement tool in Adobe Photoshop CS3 Extended software. Briefly, the image with scale bar was opened in Photoshop and the scale bar was used as reference to measure the number of pixels. The measurement tool was used to draw a line across the width from one end to the capsule to other end, and the lengths were tabulated. A similar measurement strategy was used to determine the lens epithelial sheet length. Briefly, using scale bar as reference, a line was drawn on 10× sagittal sections, with the start point being an epithelial cell adjacent to one showing signs of elongation and extending to the other end, to an epithelial cell that is adjacent to a cell starting to elongate. For all the measurements six alternate sections were taken from the center of the lens, from three independent mouse lenses.

Statistical analysis

Where required, the Student’s t-test was performed to determine significance of differences noted between the Rac1 mutant and WT specimens using Sigma plot. Values are represented as Mean ± Standard Error of the Mean (SEM).

Results

Conditional deletion of Rac1 GTPase in the eye lens and the associated ocular phenotype

To investigate the role of Rac1 GTPase in lens morphogenesis and architecture, we conditionally deleted Rac1 by expressing Cre recombinase under the control of lens regulatory sequences using three different transgenic mouse lines. As described earlier, the Le-Cre line initiates Cre expression by embryonic day 8.75 in the head surface ectoderm that includes the presumptive lens ectoderm (Ashery-Padan et al., 2000). Within the eye, the MLR10-Cre expresses Cre lens-specifically initiating at E10.5 and being active in both the lens epithelium and fibers, while, MLR39-Cre is active only in fiber cells, initiating lens specific expression at E 12.5 (Zhao et al., 2004). Recombination of the conditional Rac1 alleles led to an expected and dramatic reduction (~90%) in Rac1 protein levels in lens total homogenates (800×g supernatant; immunoblot analysis; Fig. 1C; densitometric analysis: Fig. 1D; n=3) and the intact lens (immunofluorescence analysis, Fig 1E) of P1 Le-Cre/Rac1 and MLR10/Rac1 null mice, respectively, relative to Rac1 levels in littermate WT mice. In Fig. 1C, lanes 1 and 2 represent two independent specimens from each group. As shown in Fig.1E, Rac1 expression is suppressed in both lens epithelium (Epi) and fibers (LF) in Le-Cre/Rac1 (lens is indicated with line drawing) and MLR10/Rac1 cKO mice. Compared to the Le-Cre/Rac1 and MRL10/Rac1 cKO lenses, the MLR39/Rac1 cKO mouse lenses exhibited only a 60% reduction in Rac1 protein levels (Fig. 1C & D). As expected, this reduction in Rac1 protein level was specific to fiber cells but not noted in the epithelium (Fig. 1E). Correspondingly, while both Le-Cre/Rac1 and MLR10/Rac1 cKO (weaning and older) mice exhibited severe, bilateral microphthalmia, the MLR39/Rac1 cKO mice had eyes of normal size (data not shown). For immunoblot analyses of Rac1 protein levels in the Le-Cre/Rac1 cKO mice, intact lenses from day 1 old mice, which were found only in a small number of specimens (as shown in Fig. 1E), were used.

Histological analysis (sagittal sections) of developing lenses by hematoxylin and eosin (H&E) staining revealed morphological abnormalities in both Le-Cre/Rac1 and MLR10/Rac1 cKO mice. At E12.5, the developing lenses of Le-Cre/Rac1 cKOs were smaller in size with the primary lens fiber cells displaying delayed elongation compared to littermate WT lenses (Fig.2A, arrows). By E14.5, the lens epithelial sheet length in Le-Cre/Rac1 cKO mice becomes markedly shorter than that of WT lenses. Further, the Le-Cre/Rac1 cKO mice exhibit defective lens fiber cell organization and reduction in lens size (Fig.2A). The lens then becomes progressively and severely deformed through E15.5, E17.5 and day 1, with the lens tissue attaching to the cornea, followed ultimately by complete rupture of the lens posterior capsule and leakage of lens content into the vitreous body (Fig.2B). Considerable variability was noted with respect to severity of lens phenotype within the same line. For example, a small number of eyes derived from the Le-Cre/Rac1 cKO mice at P1 contained intact lens although with much reduced size as shown in Fig. 1E. In contrast to the Le-Cre/Rac1 cKO lenses, the MLR10/Rac1 cKO lenses showed no notable defects prior to E15.5 (not shown). At E15.5, although the lens epithelium and fiber cell elongation are normal, lens size is much smaller and primary fiber cells display abnormal orientation with respect to anterior to posterior polarity, compared to the WT (Fig. 2B). By E17.5, all the fibers were visibly disoriented compared to the WT, and by day1 (P1), the lens appears more cup-shaped as opposed to the spherical shape typical of normal lenses, with fibers exhibiting abnormal migration pattern and ultimately leading to a ruptured posterior capsule in some lenses. In both Le-Cre/Rac1 (E14.5) and MLR10/Rac1 (E17.5 and P1) cKOs however, expression of fiber cell differentiation markers including β/γ-crystallins and aquaporin-0 was found to be comparable to WT lenses by immunohistochemical and immunoblot analyses (not shown). On a relative basis, lens developmental defects were more severe, and displayed an earlier onset (by almost 2.5 to 3 days) in the Le-Cre/Rac1 cKO mice compared to the MLR10/Rac1 cKO mice, consistent with the expected earlier onset of Cre expression

in the Le-Cre/Rac1 cKO mice. In contrast, the MLR39/Rac1 cKO lenses (both neonatal and adult) did not show any observable defects in either lens development or architecture (data not shown). Based on these histological observations, we only used the embryonic (Le-Cre/Rac1 and MLR10/Rac1) and P1 (MLR10/Rac1) intact lens specimens from cKO mice along with their respective littermate WT mice for all further comparative analyses.

Rac1 deficient mice exhibit defects in lens shape, fiber cell migration, orientation and suture formation

The lenses derived from both the Le-Cre/Rac1 and MLR10/Rac1 cKO mice exhibit consistent abnormalities in lens shape, suture formation, fiber cell migration pattern and orientation with severe and earlier onset in the Le-Cre/Rac1 cKO lenses compared to the MLR10/Rac1 cKO (Figs. 2 and 3). In both Le-Cre/Rac1 and MLR10/Rac1 cKO lenses, differentiating fiber cells starting from embryonic stages (E12.5 and E15.5, respectively) fail to transition to a typical concave orientation from their initial convex orientation. These changes were easily detected in histological sections of MLR10/Rac1 cKO lenses since the initial phenotype is milder in these mice relative to the Le-Cre/Rac1 cKO lenses (Fig. 3). As shown in the schematic drawings (Figs.3A and C), early differentiating WT fibers elongate at the germinative zone, migrating in a convex orientation initially, gaining a concave orientation and migrating toward the lens interior by reorganizing their adhesive interactions posteriorly with basement membrane of the capsule and anteriorly with epithelial cells. This transition in fiber cell morphology occurs after they develop contacts with the lens epithelium through the apical terminals, and with the posterior capsule via their posterior terminals. Subsequently, these fiber cell terminals (both apical and basal) detach from the epithelium and posterior capsule, and the fiber cell terminals at the anterior and posterior poles interact with each other deriving from the opposite poles and form sutures (Kuszak et al., 2004). In the Rac1 cKO lenses (in both Le-Cre and MLR10 Rac1 cKO), the fiber cells fail to migrate, orient normally and gain the expected concave orientation (Fig. 3A–C), and to form the regular lens sutures (Fig. 3D, arrows). The extent of these defects, especially the pattern of fiber cell migration, orientation and sutures appears to vary from lens to lens as depicted in the schematics (Fig.3). These schematics represent only a small number of fiber cells of the lens. Further, in both Le-Cre/Rac1 (E14.5) and MLR10/Rac1 (P1) cKO lenses, epithelial sheet length is significantly smaller compared to the respective WT lenses based on quantitative measurements (Fig. 3E). Unlike in WT lenses, the lens epithelium in Rac1 cKOs does not extend to the bow regions or the germinative zone (Fig.3A–E). It is likely that there is a shift in the germinative zone, with the bow region shifting upwards due to the flattening of the anterior hemisphere in these Rac1 cKO lenses. These different phenotypes collectively lead to the abnormal shape of both Le-Cre/Rac1 and MLR10/Rac1 cKO lenses as depicted in the schematic drawings (Fig.3).

Increased lens epithelial and fiber cell apoptosis in the absence of Rac1 GTPase

As described above, one of the predominant phenotypes in the Rac1 deficient mice include microphthalmic eyes with reduced lens size and shortened lens epithelial sheet suggesting impairment in cell survival mechanisms (Figs. 1–3). To determine whether the absence of Rac1 GTPase impacted cell survival of both epithelium and fiber cells of the lens and led to size and shape changes in Rac1 deficient lenses as noted in Figs 1–3, we evaluated the status of apoptosis using TUNEL analysis of E14.5 Le-Cre/Rac1, E17.5 MLR10/Rac1 cKO, and corresponding WT eyes. Quantitative analysis of TUNEL positive cells (based on direct counting, n=4 independent samples counted) revealed a significant increase in apoptosis in both epithelium and fiber cells of the Le-Cre/Rac1 (red/orange staining, arrows) and MLR10/Rac1 (green/yellow, arrows) cKO lenses compared to WT lenses (Fig. 4A and B). In Fig 4A, while the Le-Cre/Rac1 specimens were counterstained for cell nuclei (blue fluorescence) with Hoechst, the MLR10/Rac1 specimens were stained with propidium

iodide (red fluorescence). The green fluorescence in the Le-Cre/Rac1 null specimens is from the GFP expression in the Le-Cre mice. The diffused green stain in the WT specimen represents nonspecific background.

Defective actin cytoskeletal organization and downregulated expression of Rac GTPase effector proteins in Rac1 cKO lenses

To determine the effects of the lack of Rac1 expression on lens epithelial and fiber cell actin cytoskeletal organization, we examined F-actin staining of lens cryosections with rhodamine-phalloidin (red fluorescence). Lenses derived from Le-Cre/Rac1 (E12.5, E14.5 and E15.5) and MLR10/Rac1 cKO mice (E15.5, E16.5, E17.5 and P1) from different age groups were used in these analyses. Both Le-Cre/Rac1 and MLR10/Rac1 cKO lenses showed a gradual and progressive reduction in F-actin staining in both epithelium and fiber cells starting from E12.5 and E15.5 in the Le-Cre/Rac1 and MLR10/Rac1 cKO lenses, respectively, as compared to WT lenses (Fig. 5). Further, F-actin fluorescence intensity quantitated (n=4) by pixel counting using ImageJ (A) or Metamorph (B) confirmed a significant reduction in the E14.5 Le-Cre/Rac1 and day 1 MLR10/Rac1 cKO lenses as compared to littermate WT lenses (presented as % change in F-actin signal intensity from WT; Fig. 5C), indicating the disruption of actin cytoskeletal organization and actin polymerization in the Rac1 deficient lenses.

To obtain further insight into the molecular basis for the changes in F-actin distribution in Rac1 deficient lenses, we assessed the expression and distribution profiles of downstream regulatory components of Rac1 signaling pathways that are known to regulate actin nucleation and branching. Expression of WAVE-2, Abi-2, and Nap1 was assessed by immunofluorescence and immunoblot analysis of either E15.5 Le-Cre/Rac1, E17.5 MLR10-Cre/Rac1 (immuno-fluorescence), or P1 MLR10/Rac1 cKO (immunoblot) lenses. Immunofluorescence staining of both WAVE-2 and Abi-2 were found to be markedly decreased in both the epithelium (Epi) and fiber cells (LF) in Rac1 cKO lenses compared to WT lenses (Fig.6A). Additionally, immunoblot analysis of P1 MLR10/Rac1 cKO intact lens homogenates (800×g supernatants) confirmed a significant decrease (n=3, pooled specimens; protein levels normalized to β-tubulin) in levels of WAVE-2, Abi-2 and Nap1 proteins compared to littermate WT lenses (Fig. 6B & C). In addition to these Rac1 effector molecules, we also evaluated for changes in phosphorylation status of cofilin in the P1 MLR10-Cre/Rac1 cKO lens homogenates (800×g supernatants). Cofilin, a well characterized downstream target of Rac GTPase signaling with actin filament severing activity and role in cell migration, is negatively regulated by phosphorylation at serine 3 (Arber et al., 1998; Huang et al., 2006; Yang et al., 1998). Therefore, changes in cofilin phosphorylation were quantified by immunoblot analysis using a phospho-specific cofilin antibody. Intriguingly, the levels of phospho-cofilin were found to be significantly elevated (by ~ 48%, n=3, pooled specimens) in the Rac1 deficient lenses compared to WT specimens (Fig. 6B & C).

Impaired cell-cell interactions in the Rac1 deficient lens epithelium and fibers

To explore the effects of absence of Rac1 GTPase on lens epithelial and fiber cell-cell interactions, we examined the distribution pattern of E-cadherin in the lens epithelium, and β-catenin, Rap1A/B, Nectin-1 and N-cadherin in the lens fiber mass by immunofluorescence analyses using Le-Cre/Rac1 (E15.5) and MLR10/Rac1 cKO (E17.5 and P1) lenses. Lens sagittal and equatorial sections were analyzed for lens epithelial and fiber cell-cell junctions, respectively. The lens epithelium of both Le-Cre/Rac1 and MLR10/Rac1 cKO specimens showed a notable reduction in E-cadherin staining at cell-cell junctions as compared to WT specimens (Fig. 7A & B). Insets in Fig. 7B depict magnified (2.5 X) areas of the central epithelium (indicated with a box). While N-cadherin, β-catenin, Nectin-1 and Rap1A/B were

distributed discretely to the cell-cell junctions of the hexagonal fiber cells (LF) in the WT specimens, these proteins did not localize to the cell-cell junctions in Rac1 deficient lenses (in E17.5 and P1 MLR10/Rac1, Fig. 7C, data shown for the P1 specimens). Additionally, the changes in cell adhesive interactions in the Rac1 deficient lenses were associated with a significant decrease in N-cadherin, β-catenin, and Nectin-1 protein levels based on immunoblot analysis of the membrane enriched insoluble fraction derived from the P1 Rac1 cKOs as compared to WT lenses (Fig. 7D & E; n=3, pooled specimens, normalized to β-tubulin protein levels of 800×g lens supernatant), indicating impaired formation and stability of adherens junctions in the Rac1 deficient lenses. Due to the severe phenotype associated with the Le-Cre/Rac1 cKOs, we could not obtain suitable equatorial plane paraffin sections for these analyses.

To explore whether the changes in the adherens junction complexes described above in the Rac1 deficient lenses influence the hexagonal geometry and symmetric organization of fiber cells, we performed transmission electron microscope-based histological analysis using equatorial sections of lenses from E15.5 Le-Cre/Rac1, E17.5 MLR10/Rac1 ckO lenses, and their respective WT lenses. As shown in Fig. 7F, the WT lens fibers showed an expected hexagonal shape with long (arrows) and short arms (arrow heads) with close packing among the adjacent fiber cells. In contrast, the Rac1-deficient lens specimens exhibited disorganized fiber cells with disrupted hexagonal cell shape (Fig.7F). These observations are based on a minimum of 3 independent analyses.

Impaired extracellular matrix synthesis and thinning of lens capsule in Rac1 deficient mouse lenses

Since a ruptured posterior capsule was one of the consistent phenotypes noted in the Rac1 deficient lenses, we examined the possible influence of Rac1 deficiency on the organization and distribution of extracellular matrix proteins (ECM) of the lens by immunofluorescence analysis. Antibodies against collagen IV, laminin and fibronectin were used to analyze E15.5 Le-Cre/Rac1 and P1 MLR10/Rac1 ckO lenses, alongside littermate WT specimens. As shown in Fig. 8A, all three antibodies revealed specific and intense staining distributing only to the lens capsule. Additionally, based on these staining patterns, in both Le-Cre/Rac1 and MLR10/Rac1 cKO lenses, we observed a consistent thinning of the posterior capsule more so than the anterior capsule, relative to WT controls. Furthermore, measurements of posterior central capsule thickness revealed a significant (by 60%) decrease in Rac1-deficient lenses compared to WT controls (Fig.8B, n=6). Additionally, Rac-deficient lenses exhibited marked reduction in immunofluorescence staining for all three ECM molecule distribution assessed (fibronectin, laminin and collagen IV), relative to WT specimens (Fig. 8A). Based on these observations, we also analyzed protein levels of collagen IV, laminin and fibronectin, in lysates (800×g supernatants) of the P1 MLR10/Rac1 cKO lenses by immunoblot analysis (Fig. 8C). Consistent with the immunofluorescence data, there were significant decreases in the levels of collagen IV, laminin and fibronectin in Rac1 deficient lenses compared to WT specimens based on densitometric analysis (Fig. 8D, n=3, pooled specimens, normalized to β-tubulin). In Fig. 8C, lanes 1 and 2 represent two independent specimens from each group.

Since the ECM organization of lens capsule, fiber cell adhesion and migration were severely impaired in the Rac1-deficient lenses (Figs.3 and 7), we then evaluated the levels of integrin proteins, which function as ECM receptors. Immunoblot analysis of lens lysates (800×g supernatants) derived from the P1 MLR10/Rac1 cKO mice showed a significant decrease in the levels of αvβ1, αvβ3, αvβ5 and β1 integrins compared to WT lenses (Fig.8E and F, n=3, pooled specimens), indicative of down regulation or degradation in association with the decreases in ECM noted in the absence of Rac1 in cKO lenses (Fig. 8).

Based on these different observations, we also evaluated the organization and interaction of fiber cell posterior terminals with the lens capsule by TEM using sagittal sections of both Le-Cre/Rac1 (E15.5) and MLR10/Rac1 (E17.5) cKO lenses along with respective WT specimens. Interestingly, both the Le-Cre/Rac1 and MRL10/Rac1 cKO lens specimens exhibited distinct morphological abnormalities at the interface of fiber cell terminals and the lens capsule basement membrane (Fig.8G). While the WT specimens showed well organized and spread out, web-like membrane/cytoplasmic extensions (Fig.8G, arrows) attaching fiber cell terminals to the lens capsule basement membrane, these web-like protrusive structures were smaller, broken and detached from the lens capsule in the Rac1 deficient specimens (Fig. 8G, arrow heads). It is not clear whether these structures are membrane protrusions of the fiber cell terminals enriched in basal membrane complexes (BMCs) known to be composed of cell adhesive proteins, β1-integrin, myosin and actin (Bassnett et al., 1999). However, there seem to be definite abnormalities in the attachment of the membrane extensions to the capsule in the Rac1-deficient lens, providing morphological evidence for the disruption in the membrane extensions and adhesive interactions between the basement membrane of capsule and the fiber cell posterior terminals. These conclusions were based on data derived from four independent specimens from each group.

Discussion

Using a tissue-specific conditional gene deletion approach, we demonstrate an essential role for Rac1 GTPase during lens morphogenesis and maturation. We show that Rac1 GTPase regulates crucial aspects of lens morphogenesis and cytoarchitecture including epithelial cell survival, fiber cell elongation, migration and adhesion. This study also reveals the critical role for Rac1 GTPase in establishment of lens shape, suture formation, capsule basement membrane integrity, and fiber cell hexagonal geometry, which are important determinants of lens function.

Rac1 is expressed uniformly throughout the mouse lens including in the epithelium and fiber cells. Lack of Rac1 expression in the developing lens resulted in abnormal lens shape and reduction in size (Figs.2 & 3), with the prominent phenotype being manifested only when Rac1 expression is deleted from both lens epithelium and fibers, as evidenced by the lack of a lens phenotype in MLR39/Rac1 cKO mice in which Rac1 expression is deleted only in the fiber cells (Figs. 1). This observation demonstrates the importance of the epithelium and its interaction with fiber cells in establishment of lens shape and growth. Further, this phenotype appears to be a direct result of shortening of the epithelial sheet, increased apoptosis, and the abnormal fiber cell migration and orientation noted in the Rac1 deficient lenses (Fig.3 & 4). While the molecular basis for the shortened epithelial sheet in Rac1 deleted lenses however, is not entirely clear at present, we speculate that the increase in epithelial cell apoptosis (Fig. 4) which is consistent with the known anti-apoptotic activity of Rac (Murga et al., 2002; Nishida et al., 1999) could be partly responsible for this phenotype. Additionally, the lens epithelium in Rac1 null mice exhibited abnormal cell cycle progression based on *in vivo* BrdU incorporation profile (Fig. S1) in association with defective E-cadherin-based cell-cell interactions, suggesting compromised cell survival and proliferation in the absence of Rac1 GTPase in lens. However, it is important to point out that the MLR39 Cre transgenic mice start expressing the Cre protein from E12.5, unlike the Le-Cre (at E8.75) and the MLR10 (at E10.5) mice. Further, the promoters driving Cre expression are different in the three Cre transgenic mice used in this study (Ashery-Padan et al., 2000; Zhao et al., 2004). Therefore, the possibility that lack of phenotype in the MLR39/Rac1 mutant mice is partly attributable to the differences in amount and onset of Cre expression in fibers cells cannot be completely ruled out. It is possible that manifestation of the abnormal lens shape and fiber cell orientation phenotype result from the absence of Rac1 GTPase expression during early embryonic lens development, perhaps before E12.5.

Rac1 GTPase has been demonstrated to control directional cell migration in various cell types via regulating cell adhesive interactions and the formation of cell membrane protrusions and lamellipodia at the leading edges, by acting downstream of growth factor receptors, integrins, PI3 kinase and its lipid products (Burridge and Wennerberg, 2004; Raftopoulou and Hall, 2004; Ridley, 2001b; Ridley et al., 2003). However, the role of Rac in cell migration in the context of organogenesis is obscure (Heasman and Ridley, 2008; Wang and Zheng, 2007), and this study provides direct evidence for the involvement of Rac1 in fiber cell migration and organization in the intact lens, as shown in Fig. 3. The mouse lens expresses both Rac1 and Rac2 (Rao et al., 2004) and it is evident from the lens phenotype and other lens changes reported in this study that Rac1 plays a non-redundant role in lens. Rac1 GTPase regulates actin polymerization during lamellipodial extension and membrane ruffle formation by activating the actin–nucleating ARP2/3 complex through WASP-family verprolin-homologous proteins (WAVE) (Eden et al., 2002; Ridley, 2011; Stradal et al., 2004; Takenawa and Suetsugu, 2007; Yamazaki et al., 2003). Importantly, WAVE-2 has been demonstrated to regulate ARP2/3 mediated actin assembly and branching in a wide range of systems, acting in concert with Sra1, Nap1, Abi and HSPC300, which exist as a complex with WAVE-2 (Eden et al., 2002; Ridley, 2011; Stradal et al., 2004; Takenawa and Suetsugu, 2007). Rac1 GTPase interacts with and activates the WAVE-2 complex through the Sra1 subunit (Kunda et al., 2003; Pollitt and Insall, 2009; Stradal et al., 2004; Takenawa and Suetsugu, 2007). WAVE-2 and Abi-2 were found to be abundantly expressed in lens fibers relative to the epithelium and other ocular tissues based on distribution analysis (Fig. 6A). Moreover, distribution analysis of actin filaments, WAVE-2 and its associated proteins Abi-2 and Nap1 demonstrated reduced actin filament staining and downregulation of WAVE-2, Abi-2 and Nap1, in the lens epithelium and fiber cells of Rac1 cKO mice, implying impairment in actin nucleation possibly via the ARP2/3 complex. These observations, taken together with the earlier report on the lens phenotype of defective fiber cell migration and cell-cell interactions in the Abi-2 null mice (Grove et al., 2004), confirm the importance of Rac1 GTPase regulated WAVE-2 complex activity in controlling fiber cell migration. Abi-1 and Abi-2 both have been found to exist as part of the WAVE protein complex and to regulate actin dynamics (Eden et al., 2002; Soderling et al., 2002).

Stimulation of PAK kinase and LIM kinase by Rac1 GTPase results in the phosphorylation-dependent inactivation of cofilin (Arber et al., 1998; Huang et al., 2006; Yang et al., 1998), and leads to decreased actin filament severing and cell movement under normal circumstances. Intriguingly, deletion of Rac1 expression did not result in the expected decrease in PAK and LIM kinase-mediated cofilin phosphorylation, with Rac1 KO lenses exhibiting an increase in cofilin phosphorylation (Fig. 6B and C). This observation suggests the involvement of a Rac1-independent pathway in the inhibition of cofilin activity in the Rac1 KO lenses. Such a pathway is likely upregulated as an adaptive response to the Rac1 deficiency-induced alterations in actin dynamics and cell mobility in the Rac1 KO lenses. We have not analyzed the status of Slingshot phosphatase activity, which is known to dephosphorylate and control cofilin activity (Huang et al., 2006), in Rac1 cKO lenses.

It is important to note that, in addition to involvement of Rac GTPase downstream signaling pathways in fiber cell actin dynamics and migration discussed above, the fact that Rac1 deficient lenses and Sfrp2 (secreted WNT antagonist) overexpressing lenses (Chen et al., 2008) appear to share a striking number of abnormalities including changes in shape, shortened epithelial sheet length, and abnormal fiber cell migration and cytoskeletal organization, further suggests that Rac1 is also an important component of the WNT/PCP signaling pathway in the lens.

Another prominent phenotype in the Rac1 deficient lenses was disorganization of fiber cells, defective suture formation and disruption of the prismoid morphology of fiber cells. Lens

suture formation depends on fiber cell migration, spreading and turnover of cell-cell adhesive interactions at the interface of apical fiber tips and epithelium, the basal tips of fiber cells and basement membrane of capsule (Kuszak, 2004), and between the lateral membranes of fiber cells. As discussed above, in addition to defective fiber cell migration, N-cadherin/β-catenin and Rap1/Nectin mediated cell-cell interactions were disrupted in the Rac1 deficient lenses. E-cadherin-based cell-cell junctions regulate Rac activity (Fukuyama et al., 2006; Kawakatsu et al., 2002; Sander et al., 1998; Yap and Kovacs, 2003) and activated Rac in turn regulates actin cytoskeletal interactions with the adherens junctions (Baum and Georgiou, 2011; Fukata and Kaibuchi, 2001), which are important for the stabilization of the adherens junctions (Baum and Georgiou, 2011; Fukata and Kaibuchi, 2001; Halbleib and Nelson, 2006; Hordijk et al., 1997; Takai et al., 2008). Similarly, Rap1/Nectin, which act upstream of Rac GTPase, collectively regulate adherens junctions in various other cell types (Kooistra et al., 2007; Takai et al., 2008). The disruption of fiber cell organization and hexagonal shape in Rac1 deficient lenses as assessed by TEM (Fig.7F) therefore implies that the deficits in N-cadherin/β-catenin and Rap1/Nectin mediated cell-cell interactions noted in these lenses likely compromise lens suture formation and cytoarchitecture. It is not clear however, why and how the levels of Rap1 and Nectin-1 are decreased in Rac1 KO lenses. It is unlikely that these changes are secondary to the primary insult since we not only used intact lenses for the analyses but also noted that the Rac1 deficient lenses derived from the MLR10-Cre mice at P1 did not exhibit the typical secondary changes such as extensive vacuole accumulation and degeneration of fiber cells, as noted for many types of cataractous lenses (Chen et al., 2008; Cooper et al., 2008; Simirskii et al., 2007).

The lens capsule is a basement membrane that surrounds and serves to control the shape, elastic and mechanical properties of the ocular lens. Additionally, the ECM components of the capsule play a crucial role in lens epithelial cell proliferation, differentiation, migration and cell adhesion via engagement of integrin receptors (Danysh and Duncan, 2009; Menko S., 2004). Interestingly, the posterior capsule was frequently ruptured very early on (embryonic and neonatal) in the Le-Cre/Rac1 and MLR10/Rac1 cKOs, a phenotype which was found to be associated with decreased content of specific ECM proteins (Fig. 8). ECM components are produced and secreted by the lens epithelium and fiber cells (Danysh and Duncan, 2009). It is possible that the absence of Rac1 GTPase activity results in impaired transcriptional activity and MAP kinase activation, (Coso et al., 1995; Etienne-Manneville and Hall, 2002; Hill et al., 1995; Minden et al., 1995) which in turn may be associated with, or partly responsible for, the altered basement membrane composition in the Rac1 deficient lenses. Indeed Rac GTPase has been shown to regulate the activity of several different matrix metalloproteases (Engers et al., 2001; Kheradmand et al., 1998). Therefore, the absence of Rac1 in lens appears to have a direct influence on ECM turnover. Importantly, expression of various integrins is downregulated at the level of protein in these Rac1 deficient lenses. Integrins regulate lens epithelial proliferation, survival and differentiation (Walker and Menko, 2009) and mediate cell adhesive interactions through fiber cell basal membrane complex and through interactions with epithelial cells (Bassnett et al., 1999; Simirskii et al., 2007; Walker and Menko, 2009). ECM and integrins regulate Rac GTPase activity and cell adhesive interactions (del Pozo et al., 2000; Hotchin and Hall, 1995; Price et al., 1998) and conversely, Rac1 and Rap1 control integrin activation and cell adhesion in certain cell types (D'Souza-Schorey et al., 1998; Vielkind et al., 2005). Therefore, the changes in the basement membrane protein organization and composition in the Rac1 deficient mice very likely play a key role in the compromised cell survival and defective fiber cell migration and suture formation noted in the Rac1 cKO lenses. Interestingly, although the absolute requirement of Rac1 in cell migration has remained somewhat questionable (Wells et al., 2004), Rac1 deficient fiber cells in intact lenses exhibit defective

cell membrane/cytoplasmic extensions required for cell adhesion and migration, similar to the effects noted in Schwann cells in the peripheral nerves (Benninger et al., 2007).

In conclusion, this study uncovers a crucial role for Rac1 GTPase activity in lens morphogenesis and architecture via regulation of epithelial cell survival, cell cycle progression, fiber cell migration, cell adhesion, and ECM synthesis. Importantly, Rac1 deficiency significantly impacts lens growth, shape, capsule thickness, cell survival and cytoarchitecture.

Highlights

1. Conditional Rac1 GTPase deficiency affects lens shape and cytoarchitecture.
2. Rac1 GTPase deficiency impairs lens sure formation, fiber cell migration and cell survival.
3. Absence of Rac1 GTPase impairs lens capsule basement membrane integrity.
4. Rac1 GTPase activity is essential for lens morphogenesis and structural integrity.

Supplementary Material

Refer to Web version on PubMed Central for supplementary material.

Acknowledgments

We thank Ying Hao for TEM histology and Corey Morris for genotyping and schematic illustrations. We thank Sam Zigler, Jr for providing the aquaporin-0 and crystallin antibodies, Herald Erickson for antibodies to fibronectin, laminin and collagen IV and Ann Marie Pendergast for Abi-2 antibody. This work was supported by the National Institutes of Health grants to P.V. Rao (EY12201 and EY018590), R.A. Lang (EY17848), and M. L. Robinson (EY12995) and by a National Eye Institute Core Grant for Vision Research (P30-EY5722).

References

Arber S, Barbayannis FA, Hanser H, Schneider C, Stanyon CA, Bernard O, Caroni P. Regulation of actin dynamics through phosphorylation of cofilin by LIM-kinase. Nature. 1998; 393:805–809. [PubMed: 9655397]

Ashery-Padan R, Marquardt T, Zhou X, Gruss P. Pax6 activity in the lens primordium is required for lens formation and for correct placement of a single retina in the eye. Genes Dev. 2000; 14:2701–2711. [PubMed: 11069887]

Bassnett S, Missey H, Vucemilo I. Molecular architecture of the lens fiber cell basal membrane complex. J Cell Sci. 1999; 112(Pt 13):2155–2165. [PubMed: 10362545]

Bassnett S, Wilmarth PA, David LL. The membrane proteome of the mouse lens fiber cell. Mol Vis. 2009; 15:2448–2463. [PubMed: 19956408]

Baum B, Georgiou M. Dynamics of adherens junctions in epithelial establishment, maintenance, and remodeling. J Cell Biol. 2011; 192:907–917. [PubMed: 21422226]

Beebe DC, Cerrelli S. Cytochalasin prevents cell elongation and increases potassium efflux from embryonic lens epithelial cells: implications for the mechanism of lens fiber cell elongation. Lens Eye Toxic Res. 1989; 6:589–601. [PubMed: 2487272]

Beebe DC, Vasiliev O, Guo J, Shui YB, Bassnett S. Changes in adhesion complexes define stages in the differentiation of lens fiber cells. Invest Ophthalmol Vis Sci. 2001; 42:727–734. [PubMed: 11222534]

Benninger Y, Thurnherr T, Pereira JA, Krause S, Wu X, Chrostek-Grashoff A, Herzog D, Nave KA, Franklin RJ, Meijer D, Brakebusch C, Suter U, Relvas JB. Essential and distinct roles for cdc42 and

rac1 in the regulation of Schwann cell biology during peripheral nervous system development. J Cell Biol. 2007; 177:1051–1061. [PubMed: 17576798]

Bokoch GM. Biology of the p21-activated kinases. Annu Rev Biochem. 2003; 72:743–781. [PubMed: 12676796]

Burridge K, Wennerberg K. Rho and Rac take center stage. Cell. 2004; 116:167–179. [PubMed: 14744429]

Cain S, Martinez G, Kokkinos MI, Turner K, Richardson RJ, Abud HE, Huelsken J, Robinson ML, de Iongh RU. Differential requirement for beta-catenin in epithelial and fiber cells during lens development. Dev Biol. 2008; 321:420–433. [PubMed: 18652817]

Chen L, Melendez J, Campbell K, Kuan CY, Zheng Y. Rac1 deficiency in the forebrain results in neural progenitor reduction and microcephaly. Dev Biol. 2009; 325:162–170. [PubMed: 19007770]

Chen Y, Stump RJ, Lovicu FJ, Shimono A, McAvoy JW. Wnt signaling is required for organization of the lens fiber cell cytoskeleton and development of lens three-dimensional architecture. Dev Biol. 2008; 324:161–176. [PubMed: 18824165]

Chow RL, Lang RA. Early eye development in vertebrates. Annu Rev Cell Dev Biol. 2001; 17:255–296. [PubMed: 11687490]

Cooper MA, Son AI, Komlos D, Sun Y, Kleiman NJ, Zhou R. Loss of ephrin-A5 function disrupts lens fiber cell packing and leads to cataract. Proc Natl Acad Sci U S A. 2008; 105:16620–16625. [PubMed: 18948590]

Coso OA, Chiariello M, Yu JC, Teramoto H, Crespo P, Xu N, Miki T, Gutkind JS. The small GTP-binding proteins Rac1 and Cdc42 regulate the activity of the JNK/SAPK signaling pathway. Cell. 1995; 81:1137–1146. [PubMed: 7600581]

D'Souza-Schorey C, Boettner B, Van Aelst L. Rac regulates integrin-mediated spreading and increased adhesion of T lymphocytes. Mol Cell Biol. 1998; 18:3936–3946. [PubMed: 9632778]

Danysh BP, Duncan MK. The lens capsule. Exp Eye Res. 2009; 88:151–164. [PubMed: 18773892]

del Pozo MA, Price LS, Alderson NB, Ren XD, Schwartz MA. Adhesion to the extracellular matrix regulates the coupling of the small GTPase Rac to its effector PAK. EMBO J. 2000; 19:2008–2014. [PubMed: 10790367]

Eden S, Rohatgi R, Podtelejnikov AV, Mann M, Kirschner MW. Mechanism of regulation of WAVE1-induced actin nucleation by Rac1 and Nck. Nature. 2002; 418:790–793. [PubMed: 12181570]

Engers R, Springer E, Michiels F, Collard JG, Gabbert HE. Rac affects invasion of human renal cell carcinomas by up-regulating tissue inhibitor of metalloproteinases (TIMP)-1 and TIMP-2 expression. J Biol Chem. 2001; 276:41889–41897. [PubMed: 11551917]

Etienne-Manneville S, Hall A. Rho GTPases in cell biology. Nature. 2002; 420:629–635. [PubMed: 12478284]

Fukata M, Kaibuchi K. Rho-family GTPases in cadherin-mediated cell-cell adhesion. Nat Rev Mol Cell Biol. 2001; 2:887–897. [PubMed: 11733768]

Fukuyama T, Ogita H, Kawakatsu T, Inagaki M, Takai Y. Activation of Rac by cadherin through the c-Src-Rap1-phosphatidylinositol 3-kinase-Vav2 pathway. Oncogene. 2006; 25:8–19. [PubMed: 16170364]

Girao H, Pereira P, Ramalho J, Quinlan R, Prescott A. Cholesterol oxides mediated changes in cytoskeletal organisation involves Rho GTPases small star, filled. Exp Cell Res. 2003; 291:502–513. [PubMed: 14644170]

Glogauer M, Marchal CC, Zhu F, Worku A, Clausen BE, Foerster I, Marks P, Downey GP, Dinauer M, Kwiatkowski DJ. Rac1 deletion in mouse neutrophils has selective effects on neutrophil functions. J Immunol. 2003; 170:5652–5657. [PubMed: 12759446]

Grove M, Demyanenko G, Echarri A, Zipfel PA, Quiroz ME, Rodriguiz RM, Playford M, Martensen SA, Robinson MR, Wetsel WC, Maness PF, Pendergast AM. ABI2-deficient mice exhibit defective cell migration, aberrant dendritic spine morphogenesis, and deficits in learning and memory. Mol Cell Biol. 2004; 24:10905–10922. [PubMed: 15572692]

Halbleib JM, Nelson WJ. Cadherins in development: cell adhesion, sorting, and tissue morphogenesis. Genes Dev. 2006; 20:3199–3214. [PubMed: 17158740]

Heasman SJ, Ridley AJ. Mammalian Rho GTPases: new insights into their functions from in vivo studies. Nat Rev Mol Cell Biol. 2008; 9:690–701. [PubMed: 18719708]

Hill CS, Wynne J, Treisman R. The Rho family GTPases RhoA, Rac1, and CDC42Hs regulate transcriptional activation by SRF. Cell. 1995; 81:1159–1170. [PubMed: 7600583]

Hordijk PL, ten Klooster JP, van der Kammen RA, Michiels F, Oomen LC, Collard JG. Inhibition of invasion of epithelial cells by Tiam1-Rac signaling. Science. 1997; 278:1464–1466. [PubMed: 9367959]

Hotchin NA, Hall A. The assembly of integrin adhesion complexes requires both extracellular matrix and intracellular rho/rac GTPases. J Cell Biol. 1995; 131:1857–1865. [PubMed: 8557752]

Huang TY, DerMardirossian C, Bokoch GM. Cofilin phosphatases and regulation of actin dynamics. Curr Opin Cell Biol. 2006; 18:26–31. [PubMed: 16337782]

Kawakatsu T, Shimizu K, Honda T, Fukuhara T, Hoshino T, Takai Y. Trans-interactions of nectins induce formation of filopodia and Lamellipodia through the respective activation of Cdc42 and Rac small G proteins. J Biol Chem. 2002; 277:50749–50755. [PubMed: 12379640]

Kheradmand F, Werner E, Tremble P, Symons M, Werb Z. Role of Rac1 and oxygen radicals in collagenase-1 expression induced by cell shape change. Science. 1998; 280:898–902. [PubMed: 9572733]

Kooistra MR, Dube N, Bos JL. Rap1: a key regulator in cell-cell junction formation. J Cell Sci. 2007; 120:17–22. [PubMed: 17182900]

Kunda P, Craig G, Dominguez V, Baum B. Abi, Sra1, and Kette control the stability and localization of SCAR/WAVE to regulate the formation of actin-based protrusions. Curr Biol. 2003; 13:1867–1875. [PubMed: 14588242]

Kuszak JR, Zoltoski RK, Sivertson C. Fibre cell organization in crystalline lenses. Exp Eye Res. 2004; 78:673–687. [PubMed: 15106947]

Kuszak, JR.; C, MJ. The structure of the vertebrate lens. In: Lovicu, FJ.; Robinson, ML., editors. Development of the Ocular lens. Cambridge: Cambridge Univ Press; 2004. p. 71-118.

Lovicu FJ, McAvoy JW. Growth factor regulation of lens development. Dev Biol. 2005; 280:1–14. [PubMed: 15766743]

Maddala R, Deng PF, Costello JM, Wawrousek EF, Zigler JS, Rao VP. Impaired cytoskeletal organization and membrane integrity in lens fibers of a Rho GTPase functional knockout transgenic mouse. Lab Invest. 2004; 84:679–692. [PubMed: 15094715]

Maddala R, Peng YW, Rao PV. Selective expression of the small GTPase RhoB in the early developing mouse lens. Dev Dyn. 2001; 222:534–537. [PubMed: 11747086]

Maddala R, Reddy VN, Epstein DL, Rao V. Growth factor induced activation of Rho and Rac GTPases and actin cytoskeletal reorganization in human lens epithelial cells. Mol Vis. 2003; 9:329–336. [PubMed: 12876554]

Maddala R, Reneker LW, Pendurthi B, Rao PV. Rho GDP dissociation inhibitor-mediated disruption of Rho GTPase activity impairs lens fiber cell migration, elongation and survival. Dev Biol. 2008; 315:217–231. [PubMed: 18234179]

Maddala, R.; Skiba, NP.; Lalane, R.; Sherman, DL.; Brophy, PJ.; Rao, PV. Dev Biol. 2011. Periaxin is required for hexagonal geometry and membrane organization of mature lens fibers. in Press

Malliri A, Collard JG. Role of Rho-family proteins in cell adhesion and cancer. Curr Opin Cell Biol. 2003; 15:583–589. [PubMed: 14519393]

McAvoy JW. Induction of the eye lens. Differentiation. 1980; 17:137–149. [PubMed: 7004973]

Menko, S.; W, JL. Role of matrix and cell adhesion molecules in lens differentiation. In: Lovicu, FL.; Robinson., ML., editors. Development of Ocular Lens. Cambridge University Press; 2004. p. 245-260.

Minden A, Lin A, Claret FX, Abo A, Karin M. Selective activation of the JNK signaling cascade and c-Jun transcriptional activity by the small GTPases Rac and Cdc42Hs. Cell. 1995; 81:1147–1157. [PubMed: 7600582]

Mousa GY, Trevithick JR. Differentiation of rat lens epithelial cells in tissue culture. II. Effects of cytochalasins B and D on actin organization and differentiation. Dev Biol. 1977; 60:14–25. [PubMed: 561720]

Murga C, Zohar M, Teramoto H, Gutkind JS. Rac1 and RhoG promote cell survival by the activation of PI3K and Akt, independently of their ability to stimulate JNK and NF-kappaB. Oncogene. 2002; 21:207–216. [PubMed: 11803464]

Nishida K, Kaziro Y, Satoh T. Anti-apoptotic function of Rac in hematopoietic cells. Oncogene. 1999; 18:407–415. [PubMed: 9927197]

Pollitt AY, Insall RH. WASP and SCAR/WAVE proteins: the drivers of actin assembly. J Cell Sci. 2009; 122:2575–2578. [PubMed: 19625501]

Pontoriero GF, Smith AN, Miller LA, Radice GL, West-Mays JA, Lang RA. Co-operative roles for E-cadherin and N-cadherin during lens vesicle separation and lens epithelial cell survival. Dev Biol. 2009; 326:403–417. [PubMed: 18996109]

Price LS, Leng J, Schwartz MA, Bokoch GM. Activation of Rac and Cdc42 by integrins mediates cell spreading. Mol Biol Cell. 1998; 9:1863–1871. [PubMed: 9658176]

Quinlan, R.; P, A. Lens cell cytoskeleton. In: Lovicu, FJ.; Robinson, ML., editors. Development of Ocular Lens. Cambridge University Press; 2004. p. 173-187.

Rafferty NS, Scholz DL. Development of actin polygonal arrays in rabbit lens epithelial cells. Curr Eye Res. 1991; 10:637–643. [PubMed: 1914500]

Raftopoulou M, Hall A. Cell migration: Rho GTPases lead the way. Dev Biol. 2004; 265:23–32. [PubMed: 14697350]

Ramaekers FC, Boomkens TR, Bloemendal H. Cytoskeletal and contractile structures in bovine lens cell differentiation. Exp Cell Res. 1981; 135:454–461. [PubMed: 7308306]

Rao PV, Maddala R. The role of the lens actin cytoskeleton in fiber cell elongation and differentiation. Semin Cell Dev Biol. 2006; 17:698–711. [PubMed: 17145190]

Rao PV, Maddala R, John F, Zigler JS Jr. Expression of nonphagocytic NADPH oxidase system in the ocular lens. Mol Vis. 2004; 10:112–121. [PubMed: 14978478]

Ridley AJ. Rho family proteins: coordinating cell responses. Trends Cell Biol. 2001a; 11:471–477. [PubMed: 11719051]

Ridley AJ. Rho GTPases and cell migration. J Cell Sci. 2001b; 114:2713–2722. [PubMed: 11683406]

Ridley AJ. Life at the leading edge. Cell. 2011; 145:1012–1022. [PubMed: 21703446]

Ridley AJ, Schwartz MA, Burridge K, Firtel RA, Ginsberg MH, Borisy G, Parsons JT, Horwitz AR. Cell migration: integrating signals from front to back. Science. 2003; 302:1704–1709. [PubMed: 14657486]

Rivera C, Yamben IF, Shatadal S, Waldof M, Robinson ML, Griep AE. Cell-autonomous requirements for Dlg-1 for lens epithelial cell structure and fiber cell morphogenesis. Dev Dyn. 2009; 238:2292–2308. [PubMed: 19623611]

Sander EE, van Delft S, ten Klooster JP, Reid T, van der Kammen RA, Michiels F, Collard JG. Matrix-dependent Tiam1/Rac signaling in epithelial cells promotes either cell-cell adhesion or cell migration and is regulated by phosphatidylinositol 3-kinase. J Cell Biol. 1998; 143:1385–1398. [PubMed: 9832565]

Simirskii VN, Wang Y, Duncan MK. Conditional deletion of beta1-integrin from the developing lens leads to loss of the lens epithelial phenotype. Dev Biol. 2007; 306:658–668. [PubMed: 17493607]

Soderling SH, Binns KL, Wayman GA, Davee SM, Ong SH, Pawson T, Scott JD. The WRP component of the WAVE-1 complex attenuates Rac-mediated signalling. Nat Cell Biol. 2002; 4:970–975. [PubMed: 12447388]

Stradal TE, Rottner K, Disanza A, Confalonieri S, Innocenti M, Scita G. Regulation of actin dynamics by WASP and WAVE family proteins. Trends Cell Biol. 2004; 14:303–311. [PubMed: 15183187]

Straub BK, Boda J, Kuhn C, Schnoelzer M, Korf U, Kempf T, Spring H, Hatzfeld M, Franke WW. A novel cell-cell junction system: the cortex adhaerens mosaic of lens fiber cells. J Cell Sci. 2003; 116:4985–4995. [PubMed: 14625392]

Takai Y, Miyoshi J, Ikeda W, Ogita H. Nectins and nectin-like molecules: roles in contact inhibition of cell movement and proliferation. Nat Rev Mol Cell Biol. 2008; 9:603–615. [PubMed: 18648374]

Takenawa T, Suetsugu S. The WASP-WAVE protein network: connecting the membrane to the cytoskeleton. Nat Rev Mol Cell Biol. 2007; 8:37–48. [PubMed: 17183359]

Vielkind S, Gallagher-Gambarelli M, Gomez M, Hinton HJ, Cantrell DA. Integrin regulation by RhoA in thymocytes. J Immunol. 2005; 175:350–357. [PubMed: 15972668]

Walker J, Menko AS. Integrins in lens development and disease. Exp Eye Res. 2009; 88:216–225. [PubMed: 18671967]

Wang L, Zheng Y. Cell type-specific functions of Rho GTPases revealed by gene targeting in mice. Trends Cell Biol. 2007; 17:58–64. [PubMed: 17161947]

Weber GF, Menko AS. Actin filament organization regulates the induction of lens cell differentiation and survival. Dev Biol. 2006a; 295:714–729. [PubMed: 16678812]

Weber GF, Menko AS. Phosphatidylinositol 3-kinase is necessary for lens fiber cell differentiation and survival. Invest Ophthalmol Vis Sci. 2006b; 47:4490–4499. [PubMed: 17003444]

Wells CM, Walmsley M, Ooi S, Tybulewicz V, Ridley AJ. Rac1-deficient macrophages exhibit defects in cell spreading and membrane ruffling but not migration. J Cell Sci. 2004; 117:1259–1268. [PubMed: 14996945]

Yamazaki D, Suetsugu S, Miki H, Kataoka Y, Nishikawa S, Fujiwara T, Yoshida N, Takenawa T. WAVE2 is required for directed cell migration and cardiovascular development. Nature. 2003; 424:452–456. [PubMed: 12879075]

Yang N, Higuchi O, Ohashi K, Nagata K, Wada A, Kangawa K, Nishida E, Mizuno K. Cofilin phosphorylation by LIM-kinase 1 and its role in Rac-mediated actin reorganization. Nature. 1998; 393:809–812. [PubMed: 9655398]

Yap AS, Kovacs EM. Direct cadherin-activated cell signaling: a view from the plasma membrane. J Cell Biol. 2003; 160:11–16. [PubMed: 12507993]

Zelenka PS. Regulation of cell adhesion and migration in lens development. Int J Dev Biol. 2004; 48:857–865. [PubMed: 15558477]

Zhao H, Yang Y, Rizo CM, Overbeek PA, Robinson ML. Insertion of a Pax6 consensus binding site into the alphaA-crystallin promoter acts as a lens epithelial cell enhancer in transgenic mice. Invest Ophthalmol Vis Sci. 2004; 45:1930–1939. [PubMed: 15161860]

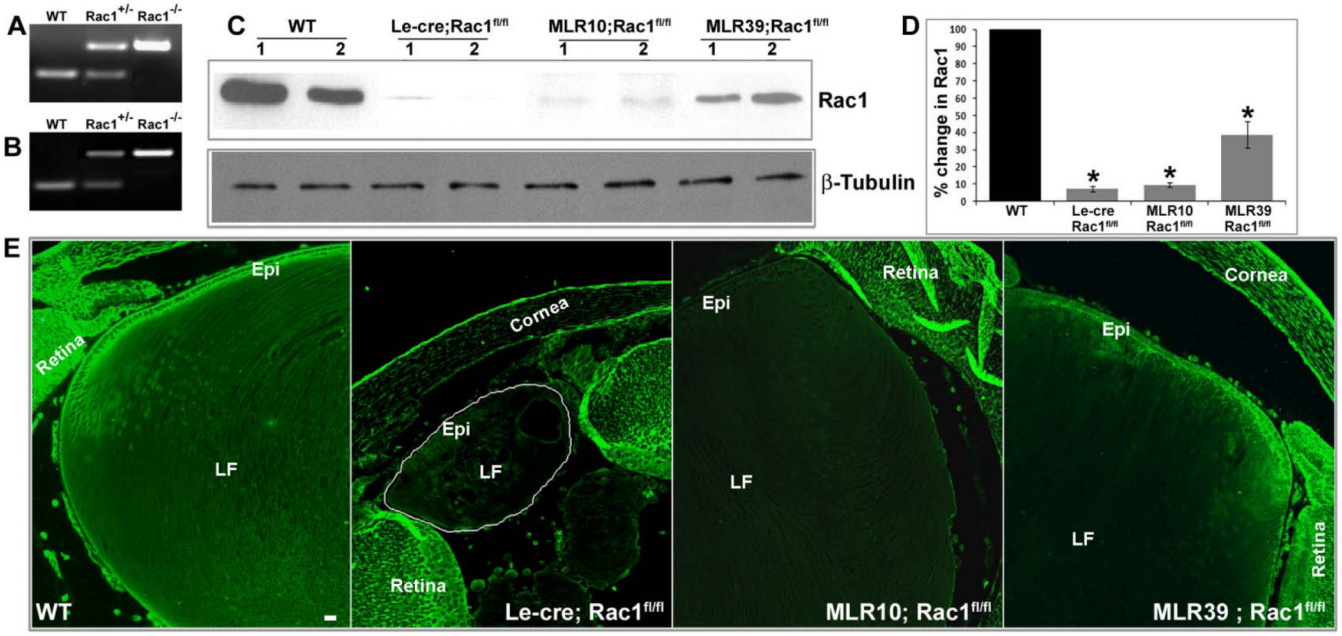

Fig. 1.

Generation of lens specific Rac1 deficient mice using the LoxP-Cre system. A and B, depict PCR based genotyping of Le-Cre/Rac1 and MLR10/Rac1 conditional mutant mice, respectively, using genomic DNA. C and D reveal a significant reduction in Rac1 protein levels in the different cKO lenses (at P1) based on immunoblot analysis (C), and subsequent densitometry based quantification (D). The values represent average ± SEM of three independent analyses (* $P < 0.05$). β-tubulin was immunoblotted (C) to confirm equal loading of protein. Lanes 1 and 2 in panel C represent two independent specimens from each group analyzed. E, Distribution of Rac1 in WT and Rac1 cKO mouse lenses based on immunofluorescence staining. Both Le-Cre/Rac1 and MLR10/Rac1 cKO lenses exhibit lack of Rac1 expression in the epithelium (Epi) and fibers (LF) relative to other ocular tissues. A line drawing in the Le-Cre/Rac1 specimen depicts the location of lens. The MLR39/Rac1 cKOs in contrast, exhibit a much reduced expression of Rac1 in lens fibers but not in the lens epithelium. Scale bar, 20μm.

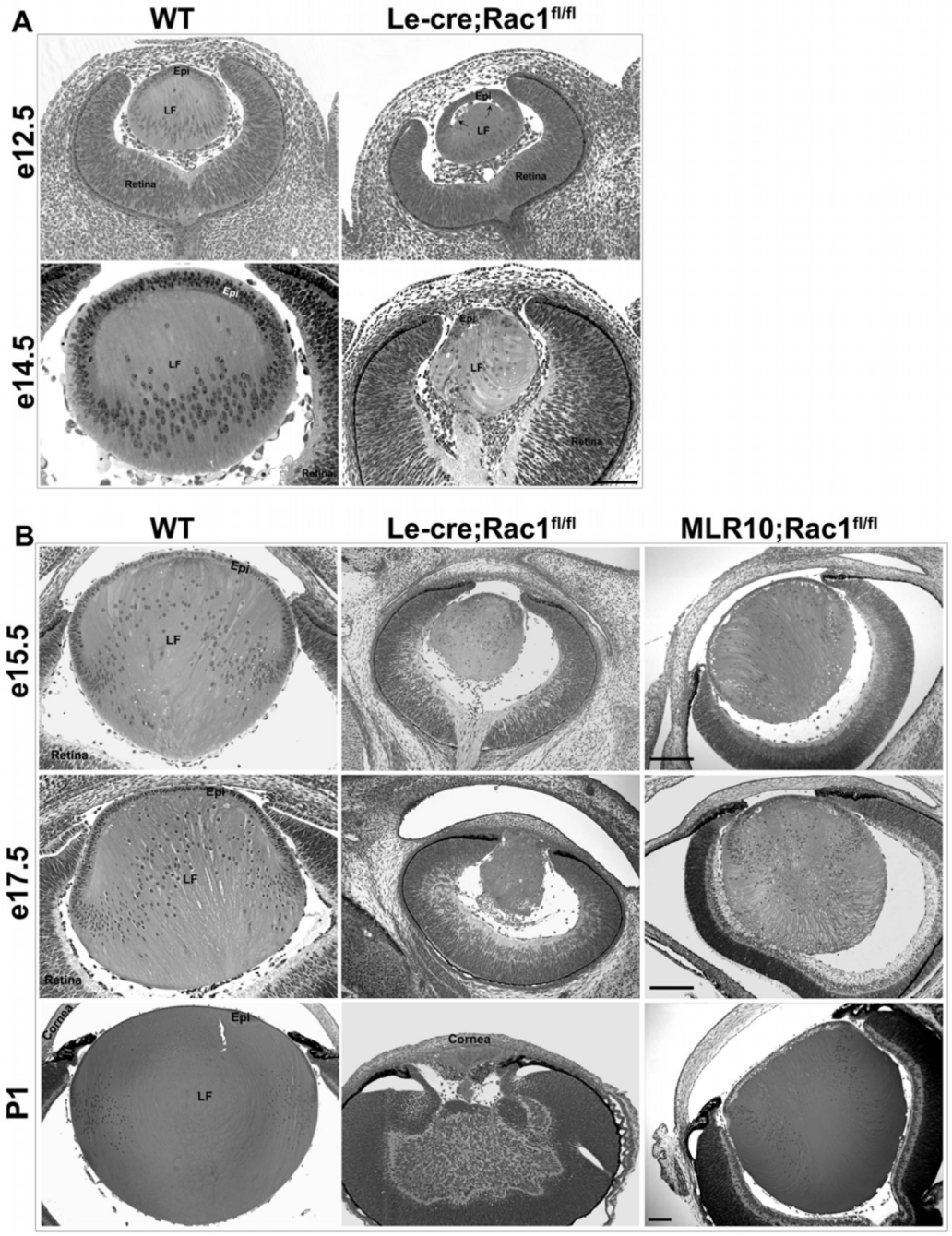

Fig. 2.

Lens phenotype in Rac1 deficient mice. A. Le-Cre/Rac1 cKO lenses exhibit reduction in size and impaired elongation of primary fiber cells (arrows) at E12.5. At E14.5, the lens epithelial sheet length becomes markedly reduced and fiber cells display abnormal organization along with abnormal lens shape in the Rac1 cKOs as compared to lenses from WT littermates. B. The Le-Cre/Rac1 cKO lenses exhibit significantly reduced size and progressive degeneration of fiber cells and lens material leaking into the vitreous body in association with ruptured capsules starting from E15.5 to postnatal day1. In contrast to Le-Cre/Rac1 cKOs, the MLR10/Rac1 cKO lenses exhibit early and noticeable histological changes starting at E15.5. At E15.5, the lens is slightly smaller and the secondary fiber cell

organization is noticeably different from the WT controls. Subsequently at E17.5 and P1, the epithelial sheet (Epi) length was found to be much shorter in the MLR10/Rac1 cKO lenses with the fiber cells (LF) exhibiting noticeable abnormalities in migration pattern and organization. These changes were found to be progressive, resulting finally in change of lens shape and size as compared to WT control lenses. Scale bars: A and B 20μm.

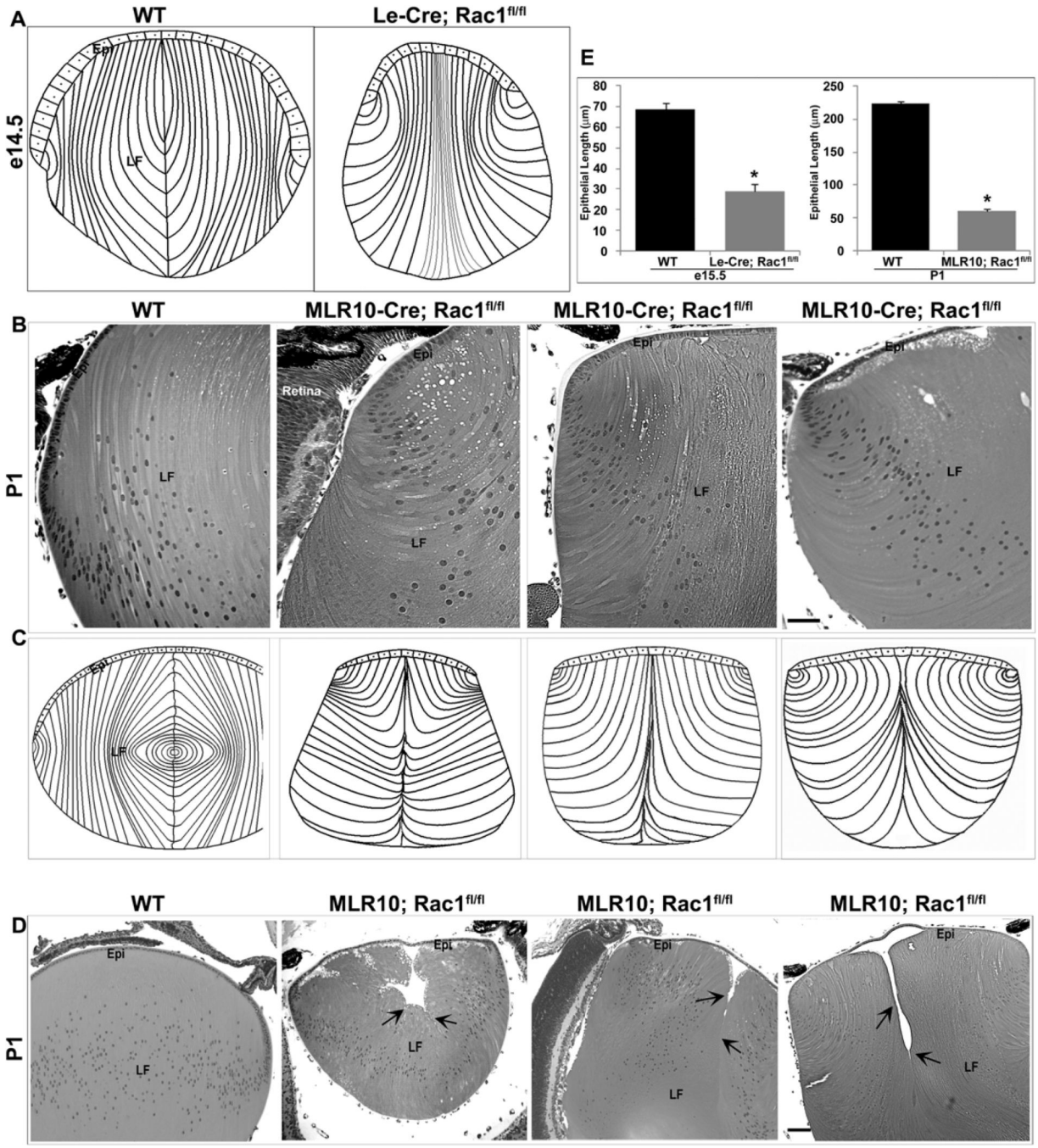

Fig. 3.

Conditional Rac1 deficient mice reveal abnormal lens shape, fiber cell migration and suture formation with considerable variations within each group. A. Schematic illustration of representative shape changes in lens and abnormal fiber cell (LF) migration pattern and shortened epithelial sheet (Epi) length in the E15.5 Le-Cre/Rac1 cKO lenses as compared to WT specimens. B and C. Representative histological images (B) and corresponding schematic drawings (C) of lens shape changes, abnormal fiber cell migration and decreased epithelial sheet length in the P1 MLR10/Rac1 cKO mice compared to WT. D. Representative histological images (D) of lenses derived from the P1 MLR10/Rac1 ckO mice exhibiting defects in suture formation (arrows) in addition to fiber cell migration. E.

Quantitative differences in lens epithelial sheet length (in μm) in Le-Cre/Rac1 and MLR10/Rac1 cKOs as compared to littermate WT lenses. Line drawings in panels A & C represent only a small number lens fiber cells. The schematics are based on 2D images. The values represent average ± SEM values from six independent specimens (* $P<0.05$). Scale bars. B and D is 20μm.

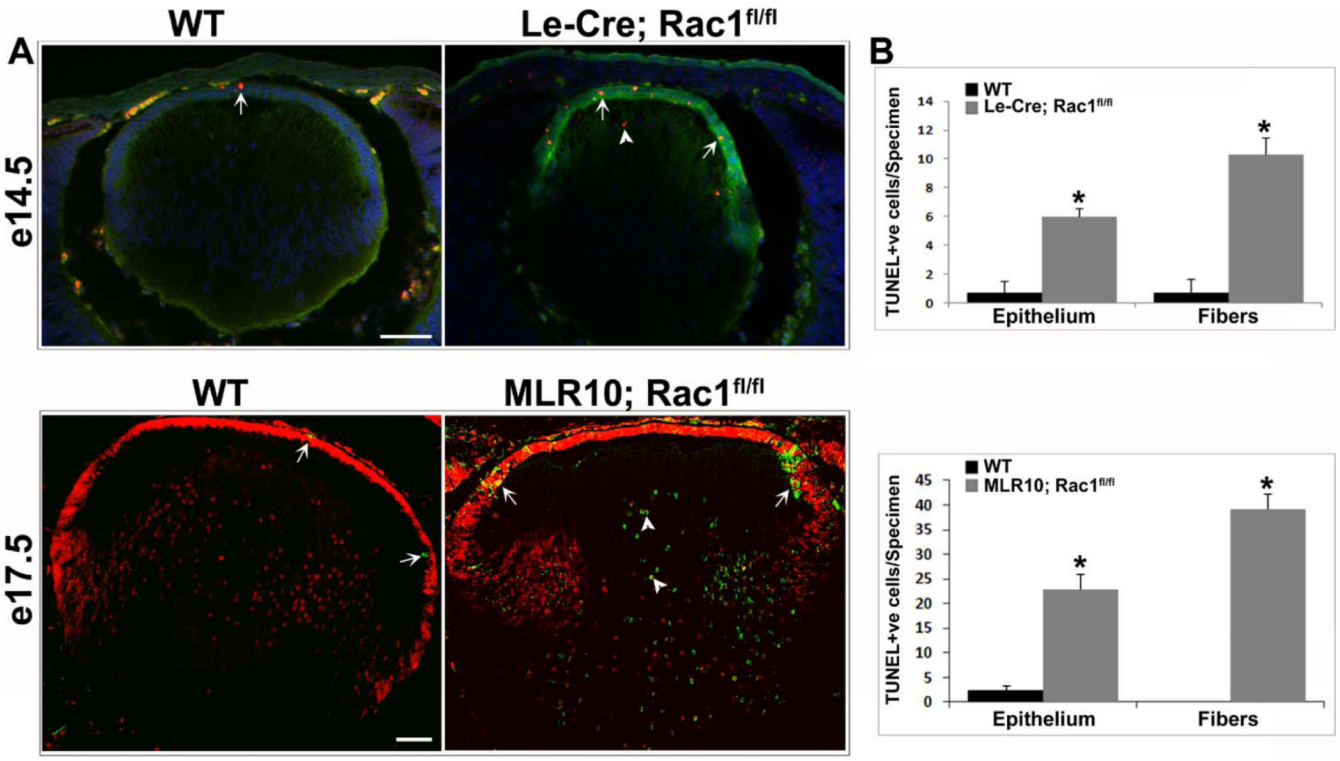

Fig. 4.

Increased apoptosis in Rac1 deficient mouse lens epithelium and fiber cells. Cryosections derived from the Le-Cre/Rac1 (E14.5) and MLR10/Rac1 (E17.5) ckO mouse lenses immunostained for TUNEL positive cells (red fluorescence in Le-Cre/Rac1 and green fluorescence in MLR10/Rac1 cKO specimens) revealed a significant increase in apoptosis in the epithelium (arrows) and fiber cells (arrow heads) compared to littermate WT lenses. The blue (top panel) and red (lower panel) staining in panel A shows nuclei counterstaining with Hoechst and propidium iodide, respectively. Green fluorescence in Le-Cre/Rac1 specimens indicates GFP distribution which in turn represents Cre expression and distribution pattern. B. Manual quantification of TUNEL positive cells (bar graphs) per specimen of lens epithelium and fiber mass showed a significant increase in both these regions in the Rac1 deficient lenses compared to the WT specimens. The values represent averages ± SEM from 4 to 5 independent analyses (*$P < 0.05$). Scale bar: Top panel: 40μm, Lower panel: 20 μm.

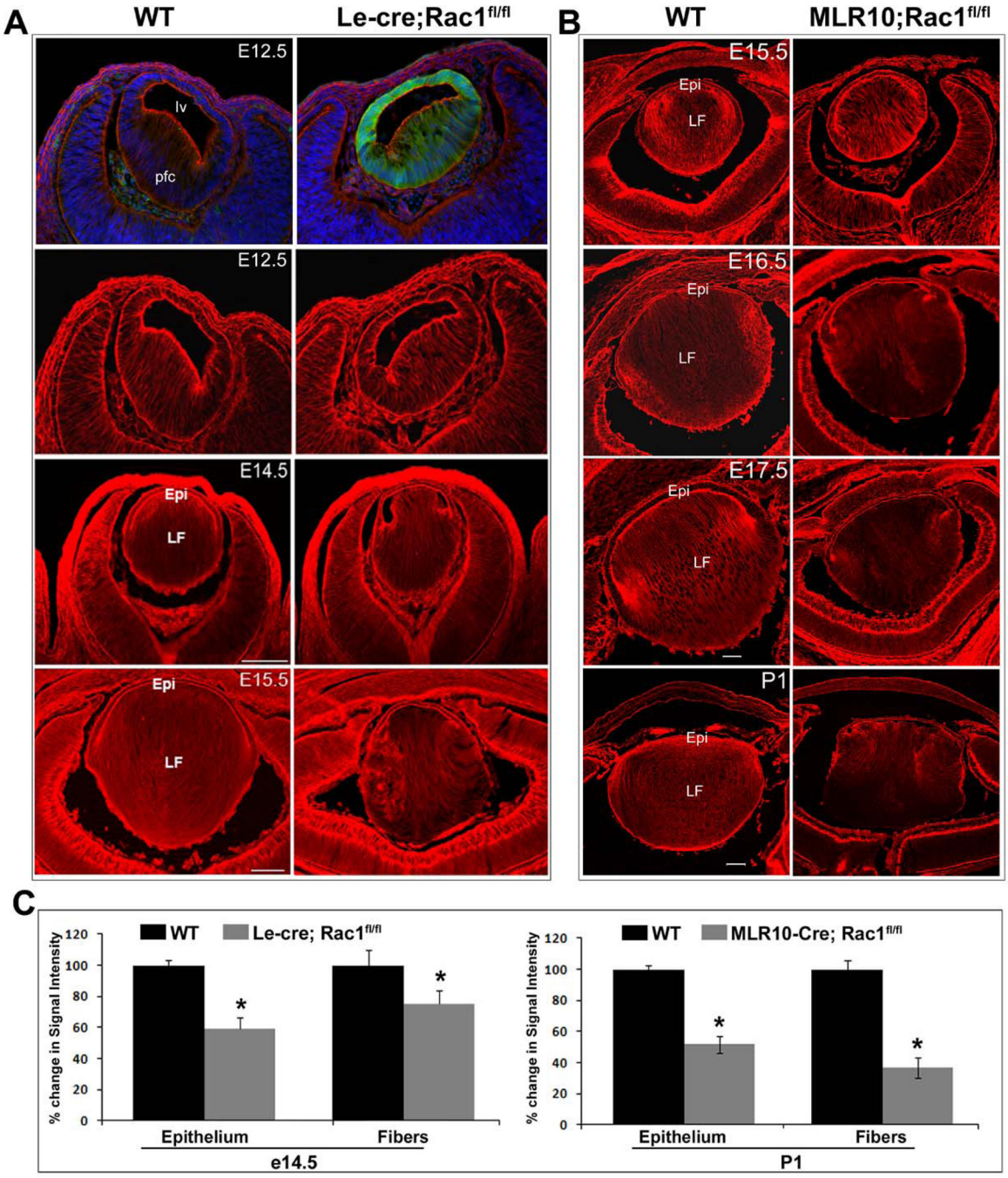

Fig. 5.

Conditional Rac1deficient mouse lenses exhibit alterations in F-actin distribution. A, B. Both Le-Cre/Rac1 and MLR10/Rac1 cKO lenses (cryosections) stained for F-actin with phalloidin- rhodamine exhibit a progressive decrease in F-actin immunofluorescence staining in epithelium (Epi) and fiber (LF) cells starting from E12.5 to day1 as compared to littermate WT specimens. C. In Le-Cre/Rac1 and MLR10/Rac1 cKO lenses at E14.5 and day1, respectively, F-actin levels were significantly decreased in both the epithelium and in fiber cells, as determined by F-actin pixel intensity measurements using ImageJ (C; Left panel) or Metamorph (C; Right panel). The values represent average ± SEM values from three independent analyses (* $P < 0.05$). Scale bars: A: 40 μm, B; 20μm. Green fluorescence

derived from the GFP in panel A shows the expression and distribution profile of Cre recombinase in the Le-Cre/Rac1 cKO lenses. Blue staining in Le-Cre/Rac1 mutant specimens show cell nuclei stained with Hoechst. lv; lens vesicle, pfc: primary fiber cells, sfc: secondary fiber cells.

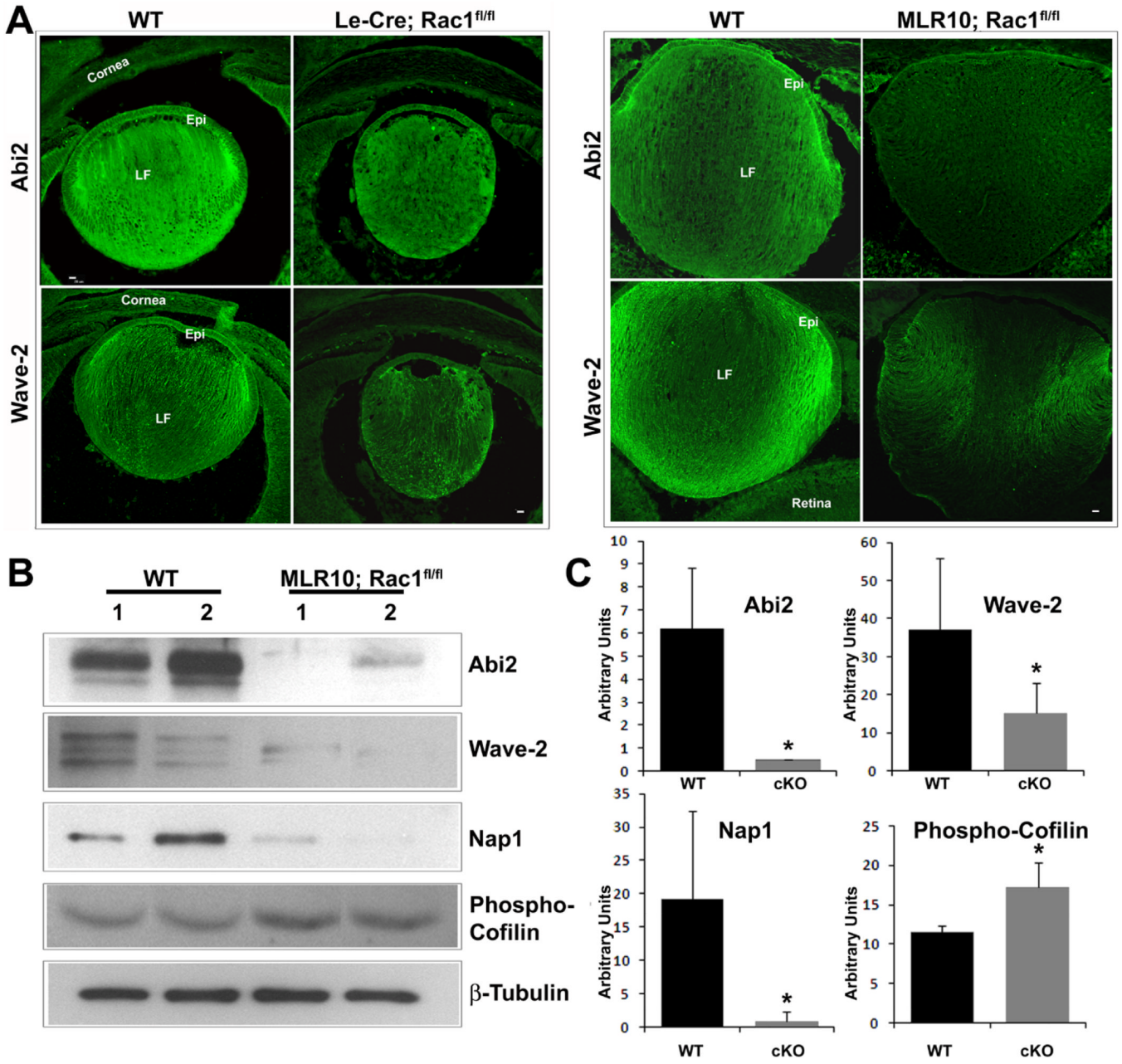

Fig. 6.

Conditional Rac1 deficient mouse lenses show abnormalities in distribution and deficits in levels of Rac1 downstream proteins involved in actin polymerization and branching A. Lens cryosections derived from the E15.5 and E17.5 Le-Cre/Rac1 and MLR10/Rac1 cKO lenses, respectively, immunostained for WAVE-2 and Abi-2 show altered distribution patterns both in the epithelium (Epi) and fiber cells (LF), with the staining being decreased relative to littermate WT lenses. B and C. Lens homogenates (800×g supernatants) derived from P1 MLR10/Rac1 cKO mice, and analyzed by immunoblotting, revealed significant decreases in levels of WAVE-2, Abi-2 and Nap1 as compared to WT lenses. In contrast, levels of phosphorylated-cofilin were increased significantly in the Rac1 deficient lenses compared to WT samples. The values represent average ± SEM values for three independent analyses (* $P < 0.05$). Scale bar: 20μm.

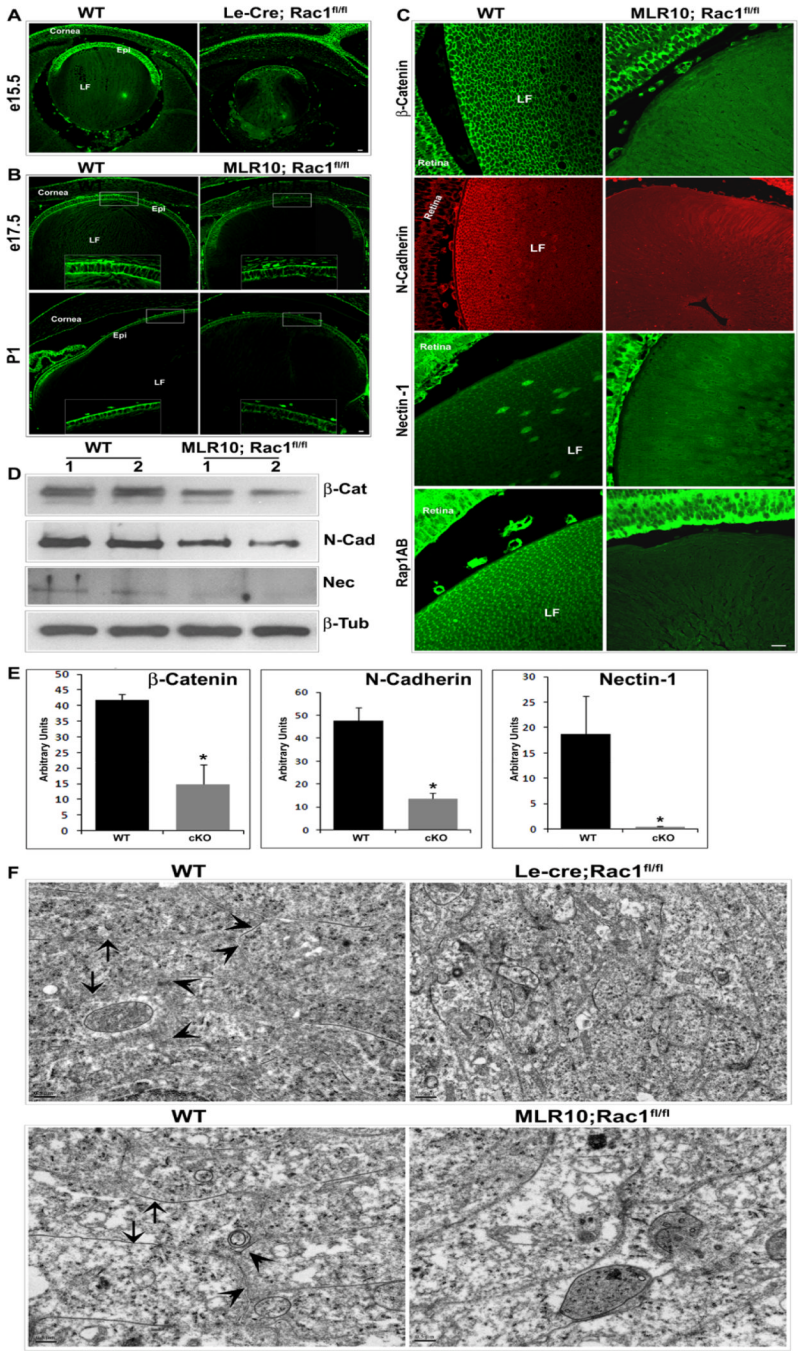

Fig. 7.

Conditional Rac1 deficient lenses exhibit defects in cell-cell interactions. A and B. Lens cryosections (sagittal plane) derived from the Le-Cre/Rac1 (E15.5) and MLR10/Rac1 (E17.5 and P1) cKO mice immunostained for E-cadherin reveal markedly reduced localization of E-cadherin to the cell-cell junctions as compared to the littermate WT, indicating disruption of adherens junctions. The insets show areas at a higher magnification (2.5×). C. Immunostaining analysis of paraffin sections of Rac1 deficient lenses (equatorial plane) from P1 MLR10/Rac1 cKO mice reveals disruption in localization of β-catenin, N-cadherin, Nectin-1 and Rap1A/B to the cell-cell junctions. These proteins are localized to the cell membrane of hexagonal fiber cells in WT but not in the Rac1 deficient lenses,

indicating defective fiber cell-cell interactions in Rac1 deficient lenses. D and E. Immunoblot and subsequent densitometric analysis, respectively, of Rac1 deficient lenses derived from P1 MLR10/Rac1 cKO mice showed a significant decrease in the levels of β-catenin, N-cadherin and Nectin-1 as compared to WT lenses. The values represent average ± SEM values of three independent analyses (* $P < 0.05$). Scale bar. A, B and C: 20μm. F. Lens equatorial sections derived from both WT and Le-Cre/Rac1 (E15.5) and MLR10/Rac1 (E17.5) cKOs were examined by transmission electron microscopy. While the WT specimens revealed closely packed fibers with distinct hexagonal shape (with two long arms and 4 short arms indicated with arrows and arrow heads, respectively), Rac1 deficient lenses exhibit disrupted fiber cell shape and asymmetric organization. Representative images of 4 independent specimens were shown. Scale bar: 0.5μm

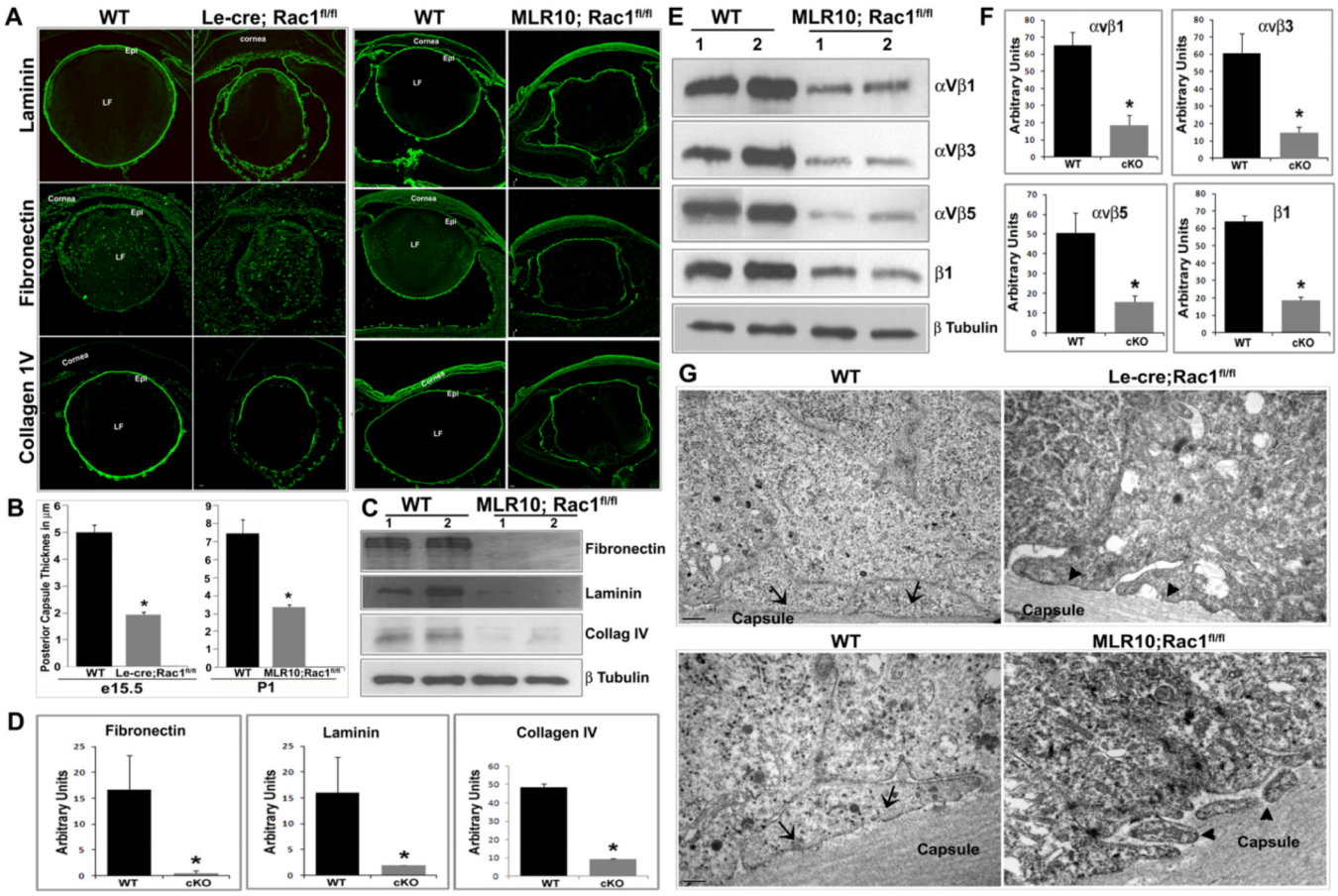

Fig. 8.

Conditional Rac1 deficient mouse lenses reveal thinning of the lens capsule in association with decreased ECM proteins and disruptions of fiber cell basal terminal attachment to the lens capsule. A. Lens cryosections (sagittal plane) derived from the Le-Cre/Rac1 (E15.5) and MLR10/Rac1 (P1) cKO mice were immunostained for various ECM proteins. Both the WT and the Rac1 deficient lenses stained positively for laminin, fibronectin and collagen IV, which localized distinctly to the lens capsule, distributing to both anterior and posterior regions. In contrast to the WT lenses however, the Rac1 deficient lenses presented with much thinner capsules, especially in the posterior region. Further, the intensity of staining of individual ECM proteins was found to be markedly reduced in the Rac1 deficient lenses relative to WT lenses. Representative images of 3 independent specimens are shown. Scale bar: 20µm. B. Quantification of posterior lens capsule (central region) thickness showed a significant decrease in both Le-Cre/Rac1 and MLR10/Rac1 cKO specimens compared to the WT lenses. C and D. Immunoblot and subsequent densitimetric analyses, respectively of ECM proteins in lens homogenates of Rac1 deficient and WT specimens confirmed a significant decrease in laminin, fibronectin and collagen IV in the P1 MLR10/Rac1 cKO lens compared to the littermate WT lens. E and F. Analysis of Rac1 deficient lenses derived from P1 MLR10/Rac1 cKO mice for changes in levels of integrins (αVβ1, αVβ3, αVβ5 and β1) by immunoblotting (E) followed by densitometric quantification (F) showed a significant decrease in the levels of these proteins as compared to littermate WT lenses. The values represent average ± SEM values from three independent analyses (* $P < 0.05$). G. Sagittal lens sections derived from the Le-Cre/Rac1 (E15.5) and MLR10/Rac1 (E17.5) cKO and corresponding WT mice assessed by transmission electron microscopy. These analyses revealed that while the fiber cell posterior membrane and cytoplasmic protrusions were

attached firmly and uniformly to the lens capsule in the WT lens images (indicated by arrows), in the Rac1 deficient lenses, the fiber cell posterior protrusions (arrow heads) were found to be shortened and broken with disrupted contacts with the lens capsule, indicating disruptions of cell-ECM interactions and impairment in fiber cell membrane protrusion. Representative images of 4 independent analyses are shown. Scale bar: 0.5μm